Regulation of nerve growth and patterning by cell surface protein disulphide isomerase

Cook, Geoffrey M.W.[1], Sousa, Catia[1], Schaeffer, Julia[1,2], Wiles, Katherine[1,3], Jareonsettasin, Prem[1,4], Kalyanasundaram, Asanish[1,5], Walder, Eleanor[1,5], Casper, Catharina[1,6], Patel, Serena[1,5], Chua, Pei Wei[1,7], Riboni-Verri, Gioia[1,8], Raza, Mansoor[9], Swaddiwudhipong, Nol[1], Hui, Andrew[1], Abdullah, Ameer[1], Wajed, Saj[1,10], Keynes, Roger J.[1]

[1]Department of Physiology, Development and Neuroscience, University of Cambridge, Cambridge, U.K.,
[2]Grenoble Institute des Neurosciences, Bâtiment Edmond J. Safra, Chemin Fortuné Ferrini, Site Santé, 38706 La Tronche Cedex, France
[3]2 More London Riverside, London, SE1 2AP, U.K.
[4]Exeter College, Turl Street, Oxford, OX1 3DP, U.K.
[5]School of Clinical Medicine, Cambridge University Hospitals, CB2 0QQ, U.K.
[6]Winter, Brandl, Fürniss, Hübner, Röss, Kaiser & Polte, Partnerschaft mbB, Patent und Rechtsanwaltskanzlei, Bavariaring 10, 80336 München, Germany
[7]School of Medicine and Health Sciences, Monash University, Jalan Lagoon Selatan, Bandar Sunway, 46150, Selangor DE, Malaysia
[8]School of Medicine, Medical Science and Nutrition, University of Aberdeen, Polwarth Building, Aberdeen AB25 2ZD, U.K.
[9]Cambridge Innovation Capital, Hauser Forum, 3 Charles Babbage Road, Cambridge CB3 0GT, U.K.
[10]University of Exeter Medical School.

Corresponding author: Roger Keynes, Department of Physiology, Development & Neuroscience, University of Cambridge, Downing Street, Cambridge CB2 3DY, U.K.
rjk10@cam.ac.uk

Abstract

Contact repulsion of growing axons is an essential mechanism for spinal nerve patterning. In birds and mammals the embryonic somites generate a linear series of impenetrable barriers, forcing axon growth cones to traverse one half of each somite as they extend towards their body targets. This study shows that protein disulphide isomerase provides a key component of these barriers, mediating contact repulsion at the cell surface in half-somites. Repulsion is reduced both *in vivo* and *in vitro* by a range of methods that inhibit enzyme activity. The activity is critical in initiating a nitric oxide/S-nitrosylation-dependent signal transduction pathway that regulates the growth cone cytoskeleton. Rat forebrain grey matter extracts contain a similar activity, and the enzyme is expressed at the surface of cultured human astrocytic cells and rat cortical astrocytes. We suggest this system is co-opted in the brain to counteract and regulate aberrant nerve terminal growth.

Introduction

Peripheral spinal nerves have a striking anatomical periodicity, or segmentation, that reflects their necessary isolation from the segments of developing bone that will form the vertebral column. This study sets out to identify the molecular basis of this patterning. We find a critical role for the enzyme protein disulfide isomerase in separating outgrowing axons from the somite cells that generate the vertebrae, and provide evidence regarding the underlying mechanism.

In avian and mammalian embryos, both outgrowing motor and sensory axons, and migrating neural crest cells, encounter the periodic somites that flank both sides of the neural tube (future spinal cord). Here they traverse preferentially the anterior (A, rostral/cranial) - rather than posterior (P, caudal) - halves of each successive

somite[1–4]. For neural crest cells this preference has been shown to depend on repulsive signalling in the P-half-somite by members of the Semaphorin/Neuropilin- and Ephrin/Eph protein families[5–9]. However the basis of axonal segmental patterning has remained elusive.

We previously identified contact repulsion as the main cellular mechanism generating axonal patterning[10,11]. Sequential repulsion of outgrowing motor and sensory axons in successive P-half-sclerotomes (future vertebrae) forces axons to traverse the anterior (A/cranial) halves. We showed that extracts of chick embryo somites cause growth cone collapse of both motor and sensory axons *in vitro*[10], a phenomenon that is widely used as a method for identifying molecules that regulate growth cone motility[12,13]. Additionally we found that the lectins peanut agglutinin (PNA) and jacalin bind selectively to the surface of P-half-sclerotome cells rather than A-half-sclerotome cells[10,14]. Immobilized PNA can be used to deplete collapse activity, and activity is recovered by lactose elution. Biochemical purification led to the identification of two PNA-binding glycoproteins shown by SDS-PAGE as two silver staining bands of 48kDa and 55kDa[10].

Results

Identification of cell surface PDI in somites

In the present work we combined PNA affinity purification with more effective inhibition of protease activity in the somite extracts, and examined the lactose eluates by semi-preparative SDS PAGE. This revealed a major silver-staining band of apparent molecular weight 57kDa, closely matching the 55kDa band seen in the earlier study[10] (*Figure 1a*). The band was excised and submitted for tryptic digestion and mass spectrometry, revealing 57 peptides distributed throughout the extent of the enzyme protein disulphide isomerase/PDIA1/P4HB (*Figure 1-figure supplement 1a*).

PDIA1/P4HB is one of a PDI-family of proteins that share in common a thioredoxin-like structural fold[15]. It is known principally as an intracellular enzyme localized in the endoplasmic reticulum (ER), where it regulates protein folding by catalyzing the formation and breakage of disulfide bonds[16–18]. A PDIA1-related molecule was also identified previously as a retina-specific candidate cell adhesion molecule[19,20]. Our finding that somite cell surface PDI (csPDI) binds PNA, and is lactose-elutable from immobilized PNA, indicates that this form of PDI is O-glycosylated. This is supported by the observation that csPDI expressed by Jurkat T cells, immortalized from human T cell leukaemia, also possesses PNA-binding O-glycans, the elongation of which can be blocked experimentally[21,22]. In addition, using a sensitive fluorescent reductase assay[23] we found that commercially purified (bovine liver) PDI does not bind to PNA-agarose, indicating that somite csPDI has an affinity for PNA based on its glycosylation state (*Figure 1-figure supplement 1b*). The expression of PDI at the surface of P-half-sclerotome cells was confirmed by live-staining of microdissected strips of chick somites, using both polyclonal anti-PDI antibody and fluorescently labelled PNA, which showed co-localization at the cell periphery in the P-half-sclerotome (Figure 1B-F). Also the onset of PNA staining in the P-half-sclerotome was found to precede the first emergence of motor and sensory axon outgrowth in the A-half-sclerotome by ~1.5-3 hours (*Figure 1-figure supplement 1c,d*)

csPDI mediates spinal nerve patterning in vivo

A role for csPDI in mediating repulsion of outgrowing spinal axons *in vivo* was tested by siRNA knockdown of csPDI expression in chick embryo somites *in ovo*, predicted to promote outgrowth of motor and sensory axons into the P-half-sclerotomes. A construct was designed on the basis of the study of Zai *et al*.[24]. They

used an antisense oligodeoxynucleotide directed against a 24 base pair target sequence in the 3' UTR of PDIA1/P4HB to show that csPDI expression in human erythroleukaemia cells is markedly reduced (>70%) without significantly affecting cell viability. The efficacy and specificity of this construct has also been shown by others[25,26]. We initially confirmed that the chick siRNA construct inhibits expression of csPDI in primary cultures of chick retinal cells and P-half-sclerotome cells (*Figure 2-figure supplement 2a-d*). PDI gene knockdown *in ovo* was then carried out by microinjection of the siRNA, incorporated in a polyethylene glycol matrix, into at least 8 somites on one side of the embryo, anterior to the most recently formed somite (stage 9-12[27]; *Figure 2a*). Confirmation of cs-PDI knockdown using Western blotting was not attempted due to the limiting availability of sufficient quantities of somite tissue, combined with the high ratio of constitutive PDI expression in the ER versus csPDI. As predicted however, PDI knockdown *in ovo* caused loss of extracellular PNA-binding in P-half-sclerotomes (*Figure 2-figure supplement 2e-g*). After siRNA injection and further incubation for 48 hours, spinal nerve outgrowth was assessed by immunohistochemistry using a neuron-specific-β-III tubulin antibody (clone TUJ1), observer-blind to treatment condition. Embryos treated with control/scrambled siRNA showed normal axon segmentation, with growth restricted to the A-half-sclerotomes (*Figure 2b*). However PDI knockdown caused outgrowing motor axons to project additionally into the P-half-sclerotomes adjacent to the neural tube/spinal cord (*Figure 2c,d*), an abnormal trajectory not seen in untreated embryos or in those similarly treated with control/scrambled siRNA. Control experiments showed that expression of the A-half-somite polarity determinant gene *Tbx18* was unaffected by siRNA injection, whereas expression of the P-half determinant gene *Uncx4.1* was variably diminished in the treated region (*Figure 2-figure supplement 2h*). Since *Tbx18* expression did not alter correspondingly, this was unlikely to be due to a P-to-A switch in cell identity, or to reflect a change in cell viability due to reduced PDI expression. It may be explained if csPDI knockdown in P-half-sclerotome cells at the A/P boundaries causes some to mix with neighbouring A-half cells and down-regulate *Uncx4.1* expression as a result. Injection of scrambled siRNA did not cause detectable sclerotome caspase-3 expression.

To rule out the possibility that these phenotypes resulted from an off-target effect of the siRNA, control experiments confirmed that co-injection of siRNA with a FLAG-M1-epitope-tagged plasmid expressing human PDIA1/P4HB (>90% homologous to chicken PDIA1[28]) rescued the normal segmented axon phenotype (*Figure 2-figure supplement 2i-k*). We also found that inhibiting the enzyme activity of PDI caused a similar phenotype. PDI possesses two independent active sites, and the small molecule PACMA 31 has been shown to form a covalent bond with a cysteine residue of the second active site, thereby inhibiting its catalytic activity[29]. PACMA 31 was applied *in ovo* using two delivery methods. First, as described above for siRNA delivery, PACMA 31 in solution (200μM) was injected directly into somites *in ovo* and the resulting axon phenotype assessed by immunohistochemistry. PACMA 56, an inactive substituted alkynyl derivative of PACMA 31 that does not bind to PDI[29], acted as a control. Consistent with the results of siRNA knockdown, PACMA 31 injection also caused abnormal axon projections into P-half-sclerotome whereas control/PACMA 56 injection did not (*Figure 2-figure supplement 2l-n*). In addition the A-P width of ventral roots increased after PACMA 31 injection, indicating axon defasciculation (*Figure 2-figure supplement 2o*).

The second PACMA delivery method involved impregnation of Affi-Gel Blue agarose beads (25-50μm diameter) with PACMA 31 or PACMA 56 (500μM), followed by microsurgical implantation of single beads *in ovo* between the neural tube and newly-formed sclerotome in stage 12-14 chick embryos. After further incubation for 24-36 hours, axon trajectories were assessed in the implant region by whole-mount immunohistochemistry. As with siRNA knockdown, PACMA 31 caused abnormal

axon outgrowth into P-half-somite territory (*Figure 2e,f*; 14/29 embryos). Using PACMA 56 as control, only an occasional axon outgrowth abnormality (1/20 embryos) was observed; in 19/20 embryos, axons were confined to the A-half-sclerotomes as in normal embryos (*Figure 2g*).

csPDI mediates axon repulsion via nitric oxide signalling/S-nitrosylation

To elucidate the mechanism of action of csPDI we first tested whether PDI causes growth cone collapse by direct interaction with the growth cone surface. The purified bovine enzyme incorporated in liposomes was added at a range of concentrations (25-1000ng/ml) to cultures of chick embryo dorsal root ganglia (DRGs) extending sensory axons on laminin in the presence of nerve growth factor (NGF). However this did not increase collapse above the control levels (0-20% of growth cones) seen after addition of phosphate-buffered saline (PBS) or untreated liposomes (*Figure 3a*).

Nitric oxide (NO) has been shown to elicit growth cone collapse *in vitro* when released in solution from a NO donor (3-morpholino-sydononimine, SIN-1)[30]. Moreover Zai *et al*.[24] have shown that NO entry into csPDI-expressing human erythroleukemia cells involves a transnitrosation mechanism catalyzed by the enzyme. Physiological NO donor S-nitrosothiol (SNO) levels have been estimated in human cerebrospinal fluid and plasma at low micromolar concentrations (respectively 0.86 ± 0.04μM[31] and 1.77±0.32μM[32]). We therefore tested whether application of PDI in combination with S-nitrosoglutathione (GSNO, 1μM) as NO donor causes growth cone collapse. Whereas application of GSNO alone in solution did not elicit collapse above control levels, significant collapse was observed when GSNO was first combined with PDI (125ng/ml) and then added to DRG cultures (~60% growth cones collapsed after 1h, *Figure 3b*). To confirm that PDI+GSNO-induced collapse in solution is reproduced in the liposome-based collapse assay, we found that the PDI concentration dependence of collapse was similar in both cases. (*Figure 3-figure supplement 3a,b*). Also the time course of PDI+GSNO-induced collapse was similar to that induced by somite extracts, and contrasted with the more rapid onset of collapse induced by the soluble repellent Sema3A (*Figure3-figure supplement 3c-e*).

We next tested the PDI inhibitors purified-bacitracin[33], anti-PDI neutralizing antibody, phenylarsine oxide (PAO)[34], acetylated triiodothyronine (T3)[35] and 16F16[36] on PDI+GSNO-induced collapse when applied in solution. Of these, three inhibitors (bacitracin, neutralizing antibody and PAO) were most effective in reducing collapse when incorporated in liposomes with PDI (*Figure 3-figure supplement 3f-k*). With the publication of the small molecule PDI-inhibitor PACMA 31 and its control PACMA 56[29], the candidacy of csPDI in mediating somite extract (SE)-induced collapse was further confirmed using PACMA 31 in liposomes, which inhibited collapse by >50% whereas PACMA 56 was inactive (*Figure 3c*).

PDI has two active sites, each with the amino acid sequence WCGHCK. Sliskovic *et al*.[37] have shown that PDI can be S-nitrosylated (PDI-SNO), and that the enzyme can also act as a denitrosylase resulting in $NO^{\cdot}$ release as a free radical. They have proposed that PDI-SNO is denitrosylated by a one-electron reduction mechanism at the second active site. Moreover they showed that glutathione (GSH) is the most effective reducing agent, and that no significant denitrosylation is observed using reducing agents dithiothreitol (DTT) or L-homocysteine[37]. Consistent with their study, we found that when PDI+GSNO or somite extracts were incorporated in liposomes and subsequently treated with GSH (3mM), collapse activity was lost. However identical experiments using 3mM DTT or L-homocysteine did not affect collapse activity. Notably, GSH did not block collapse when applied at 3μM, within the extracellular concentration range typically present *in vivo* and 3 orders of magnitude below the ambient intracellular concentration range[38] (*Figure 3d*; see Discussion). Also consistent with the observations of Sliskovic *et al*.[37], somite extract-induced collapse was inhibited by 3mM GSH but not by 3mM L-homocysteine (*Figure 3e*).

Further evidence that a NO-based mechanism elicits growth cone collapse was provided by the finding that myoglobin, regarded as a pseudo-enzymatic NO scavenger[39,40], inhibited collapse induced by PDI+GSNO and by somite extracts (*Figure 3f*). PDI+GNSO-induced collapse was also inhibited by the membrane-impermeable NO-scavenger carboxy-2-Phenyl-4,4,5,5-tetramethylimidazoline-1-oxyl 3-oxide (C-PTIO; *Figure 3g*). Somite extract-induced collapse was additionally prevented by pre-treatment of DRGs with the neuronal nitric oxide synthase (nNOS) inhibitor L-NAME, but not by its control/chiral isomer D-NAME, indicating a role for nNOS activity in the collapse process (*Figure 3h*).

These experiments implicate NO signalling in somite-induced growth cone repulsion. The *in vitro* study of Stroissnigg *et al*.[41] has likewise shown a role for S-nitrosylation of the microtubule-associated protein MAPB1 in mediating mouse DRG growth cone collapse caused by stimulation of nNOS by the calcium ionophore calcimycin/A23187. They showed further that S-nitrosylation of Cys 2457 in the MAP1B light chain sub-unit (LC1) is a critical event in the cytoskeletal dynamics underlying collapse. To examine expression of S-nitrosylated proteins in somites, we therefore carried out Western blotting of cell-free somite extracts using iodoTMT^{TM} reagent, which gives lower background labelling compared with biotin labelling. The assay was prepared from 650 dissected somite strips homogenised in HENS buffer. Remarkably only one major band (molecular weight 38kDa) was detectably S-nitrosylated (*Figure 3i*). We additionally confirmed, by Western blotting using a mouse monoclonal antibody against amino acids 2257-2357 in LC1 of mouse MAP-1B (see Methods), that this S-nitrosylated somite protein reacts strongly with the anti-LC1 antibody (*Figure 3j*). Also the nNOS inhibitor L-NAME inhibited both S-nitrosylation of the 38kDa protein (*Figure 3k*) and somite extract-induced growth cone collapse (*Figure 3h*), while the control stereoisomer D-NAME was without effect (*Figure 3h,k*). These findings indicate that a molecular mechanism similar to that proposed by Stroissnigg *et al*.[41]operates within the growth cone during its repulsion by somites *in vivo*.

csPDI activity in mammalian forebrain grey matter

We previously found that, as for somites, extracts of adult mammalian and chicken forebrain grey matter also cause sensory/DRG axon growth cone collapse that can be depleted by the use of immobilized PNA. This suggested that a contact-repulsive system similar to that in somites may be expressed in the mature CNS[42]. In confirmation we found that immobilized jacalin, a lectin that binds the same O-linked disaccharide (Galβ1-3GalNac) as does PNA, but unlike PNA is not selective for its de-sialylation, can be used to deplete collapse induced by rat forebrain extracts (RFE; *Figure 4-figure supplement 4a*). Ghosh and David[43] have also described a growth cone collapse-inducing activity in membrane preparations of rat cerebral cortical grey matter. We therefore tested whether, as for somite extracts, a range of inhibitors of PDI activity block RFE-induced collapse, and found this was the case. Application of PACMA 31 (5μM) significantly reduced collapse (by 50-60%) whereas PACMA 56 (5μM) did not (*Figure 4a, Figure 4-figure supplement 4b*). Another small molecule PDI-inhibitor, quercetin-3-O-rutinoside[44] inhibited RFE-induced collapse when used at both 1μM and 50μM (*Figure 4b*). RFE-induced collapse activity was immunodepleted using polyclonal anti-PDI antibody but not using IgG or bovine serum albumin (BSA) as sham protein controls (*Figure 4c*). Moreover, as for somite extracts, application of 3mM GSH reduced RFE-induced growth cone collapse, whereas 3mM DTT, 3mM L-homocysteine (L-HC) or 3μM GSH did not (*Figure 4d*). At GSH concentrations between 3μM and 3mM, inhibition of collapse increased with concentration (*Figure 4-figure supplement 4c*). Last, and again consistent with a NO-based mechanism, we confirmed that application of the NO scavengers myoglobin and C-PTIO depleted RFE-induced collapse (*Figure 4-figure supplement 4d,e*).

One source of csPDI in the brain may be the astrocyte, which shares fate specification by the transcription factor SOX9 with P-half-sclerotome cells (future vertebral cartilage)[45–47]. In support of this, live-staining experiments showed that csPDI is expressed on the surface of cultured human astrocytic cells, as for P-half-sclerotome cells (*Figure 4e*). Moreover extracts of these cells caused growth cone collapse that was removed by the use of immobilized PNA and jacalin (*Figure 4-figure supplement 4f*), and a cell surface preparation isolated from rat primary cortical astrocytes was found to contain csPDI (*Figure 4-figure supplement 4g*).

Collectively these experiments indicate that csPDI is a major component of the growth cone collapse-inducing activity detectable in the grey matter of the mature mammalian brain. The NGF-dependent primary sensory neurons assessed here project axons *in vivo* in the CNS as well as PNS, making synapses in the dorsal horn of the spinal cord and in the brainstem. We have shown previously that two populations of CNS-restricted neurons are also responsive to the somite contact-repellent system. When explants of embryonic day-4 (E4) chick telencephalon or E7 retina are grafted *in ovo* in place of chick spinal cord, their axons avoid P-half-somites[42,48]. Moreover chick retinal axon growth cones collapse in response to somite extracts *in vitro*[48], and in further confirmation we found that they collapse in response to PDI+GSNO (*Figure 4-figure supplement 4h*).

Discussion

The significance of PDI as an ER-based foldase/isomerase is well known, but the biological role of csPDI is less clear-cut. It has been implicated in processes such as platelet aggregation and thrombosis, and in animal cell infection by a variety of micro-organisms[17]. Here we have identified a key function for csPDI in contact repulsion using a biological system. Consistent with its location at the cell surface, somite csPDI is an O-glycosylated protein, as shown by our lectin-binding studies[10] and by Bi *et al.* for human Jurkat T cells[21]. In keeping with this, it has been shown that contact between a single DRG growth cone filopodium and the surface of a P-half-somite cell *in vitro* is sufficient to initiate a rapid filopodial withdrawal/repulsive response, followed by reorientation of the growth cone away from the cell[49]. The rapid nature of this response, combined with our finding that somite extract collapse-inducing activity is depleted using the lectins PNA and jacalin[10], argue strongly that repulsion is likely to arise from the activity of csPDI rather than ER-based PDI. These lectins have specificity for O-glycans that are synthesised and linked to protein in the Golgi apparatus before the glycoprotein is transported to the cell surface. Also consistent with a repulsion mechanism, inhibition of PDI activity *in vivo*, using either siRNA knockdown or PACMA 31 inhibition of enzyme activity, causes axons to traverse the P-half-somites. Since PDI is a multifunctional enzyme operating both within and outside cells, it is possible that this phenotype might arise for other reasons. However we used the same target for gene knockdown experiments as used by Zai *et al*.[24], who showed that cell viability is unperturbed despite inhibition of csPDI expression. Additionally we saw no change in somite morphology despite loss of lectin binding at the cell surface.

In chick somites the onset of csPDI expression in P-half-sclerotome immediately precedes the first emergence of spinal axons in the A-half. This matches well the proposed function of csPDI in mediating contact repulsion of outgrowing motor and sensory axons. The selective migration of neural crest cells in A-half-sclerotomes, which precedes by several hours the first axon outgrowth at each segmental level in the chick embryo, is likewise matched temporally by the onset of expression of the diffusible repellent Sema3F in newly-formed P-half-sclerotomes[5]. This implies that segmental patterning of neural crest cells and axons is regulated predominantly by distinct molecular signals. Supporting this, the Eph-family receptor tyrosine kinase EphB2 and its ligand ephrin-B1 have been additionally implicated in somite-based

repulsion of neural crest cells[7], but have been shown not to be necessary for motor axon segmentation[8]. The persistence of segmented spinal nerve patterning seen in both compound Neuropilin1/2 mutant mice[9,50], and in ephrin-B mutant mice[6], may therefore be explained if disrupted neural crest-repulsive signalling in these mice is compensated by segmental csPDI expression.

The models of Zai *et al.*[24] (using human erythroleukaemia cells), Ramachandran *et al.*[51] (using fibroblasts and endothelial cells) and Sliskovic *et al*.[37] have been proposed to explain how NO entry into these cells is regulated by a transnitrosation mechanism facilitated by csPDI. These *in vitro* cellular models are directly applicable to the axon growth cone/somite system *in vivo*. We suggest that csPDI acts as a de-nitrosylase, operating constitutively at the P-half-somite cell surface to promote the transfer of $NO^{\cdot}$ from extracellular S-nitrosothiols into the cytosol of contacting growth cone filopodia, thereby initiating repulsion/collapse. Extracellular S-nitrosoglutathione (GSNO) may provide a ubiquitous source of NO donor, as suggested for csPDI activity in the context of platelet aggregation[52]. Critically we have shown that its ambient extracellular concentration *in vivo* (~1μM) is sufficient, in combination with purified PDI, to elicit growth cone collapse *in vitro*. Alternatively or additionally, other NO donors may be involved.

The transnitrosation model is well supported by the finding that DRG/sensory axon growth cones collapse when exposed *in vitro* to 3-morpholino-syndoninime (SIN-1), which spontaneously dissociates in solution to release NO[30]. SIN-1-induced collapse is prevented by the presence of haemoglobin, which binds released NO[30], and we have shown that both myoglobin, which similarly binds released NO, and the membrane-impermeable NO-scavenger PTIO[53] deplete the collapse-inducing activity of somite extracts. Moreover nNOS inhibition by L-NAME prevents such collapse, indicating that NO signalling may be further amplified in the growth cone by nNOS activity.

How might NO signalling in the growth cone influence the cytoskeleton? Our results accord well with the proposal of Stroisnigg *et al*.[41] that, in axons extending *in vitro,* growth cone retraction is counteracted by a microtubule/dynein-based system. S-nitrosylation of LC1 induces a conformational change that enhances binding of the LC1-HC complex to microtubules, so blocking dynein action and promoting retraction over extension. Correspondingly, in the somite system *in vivo* both motor and sensory axon growth cones extending at the A/P-half-somite boundaries will make filopodial contact with P-half-somite cells expressing csPDI, triggering NO-mediated repulsive signalling. Consistent with this, using the iodo-TMT reagent we find that LC1 is the only S-nitrosylated protein detected in cell free extracts of dissected somite strips, which necessarily include growth cone proteins.

The observation that a repellent activity closely similar to the somite system is expressed in mammalian forebrain grey matter is of particular interest, and extends the range of brain proteins originally identified as developmental axon repellents[13,54]. Collapse-inducing activity is significantly reduced using the lectins PNA and jacalin (this study and Keynes *et al*.[42]), and is also prevented using a variety of small molecule inhibitors (PACMA 31, rutinoside, GSH) as well as myoglobin and anti-PDI antibody. Our findings additionally implicate the astrocyte as a source of this activity, since human astrocytic (1718) cells and rat cortical primary astrocytes express csPDI, and 1718-cell-derived growth cone collapse activity is removed by immobilized PNA and jacalin. In view of the involvement of NO/S-nitrosylation signalling in the csPDI-mediated repulsion mechanism, rather than a protein-based ligand-receptor interaction, a broad range of CNS axon types may prove susceptible to it. And consistent this, we have shown previously that chick CNS (retinal and telencephalic) axons respond to the somite repellent *in vivo*[42,48]. It may also be significant that csPDI expression by human malignant glioblastoma cells has been related to their invasiveness within the brain[55].

The neuron may be another source of brain-derived csPDI, since a recent proteomic analysis of CNS synaptic cleft proteins identified csPDI/P4HB among the most enriched candidates at both excitatory and inhibitory synapses in embryonic rat cortical neuronal cultures[56]; csPDI has also been identified at the surface of both neuroblastoma cells[57] and retinal cells [20]. Together with the experiments reported in this study, these findings collectively raise the possibility that csPDI is 'bifunctional' in promoting both adhesive and repulsive neuronal/glial interactions in the CNS.

In sum, this study reveals a novel role for the multifunctional enzyme PDI in the periodic patterning of peripheral spinal nerves, ensuring their separation in somites from developing cartilage and bone. The additional expression of csPDI at the astrocyte surface, and its function in repelling growing nerve terminals, suggest a promising candidate for regulating axon growth and plasticity that may be widely distributed in the developing and mature nervous system.

Methods

Chick embryo grafting procedure

Fertilized hens' eggs (Gallus gallus, Bovans Brown variety; Winter Egg Farms, Fowlmere, Cambridgeshire) were incubated at 38°C to obtain embryos at stage 12-14[27] (16-22 somites). Eggs were windowed and 0.2-0.5mL of a 1:10 mixture of India ink (Fount India, Pelikan) and phosphate-buffered saline (PBS) was injected into the sub-blastodermal space. The window was lined with silicone grease, and the embryo raised to the level of the shell by pipetting PBS into the egg through the window, creating a bubble of PBS held in place by the grease. An incision was made between the neural tube and newly-formed sclerotome on one side of the embryo, and a single Affi-Gel Blue agarose gel bead (BioRad, Cibacron blue coupled to agarose, 30-50μm diameter) impregnated with PACMA31 or PACMA56 (500μM in PBS) was implanted into the resulting space (adjacent to the neural tube medially and notochord ventrally). Embryos were then re-incubated for 24-36h before fixing and processing for axon staining (see below) as whole-mounts or as (left and right) half-embryo-mounts. PACMA31 or PACMA56 solution was made by adding 0.5ml dimethylsulfoxide to 2.2mg PACMA to make a 10mM stock solution. This was diluted x20 in PBS to make a 500μM working solution, in which the Affigel beads were then placed for 2-3h at 21°C prior to implantation.

Preparation of tissue extracts

Stage 16-18 chick embryo trunks (comprising ectoderm, somites with DRG neurons, and motor axons, neural tube and notochord) or somite strips (ectoderm, somites with DRG neurons and motor axons) were dissected and immediately placed on solid CO_2 and transferred to -80°C for longer storage. Trunks from ~60 embryos were homogenised in 1ml solubilisation medium [2%w/v CHAPS in PBS made 1mM with sodium orthovanadate and 1 tablet cØmplete protease inhibitor cocktail (Roche) per 50ml of solution] on wet ice by shearing through a 20G then 26G needle. Further homogenisation was carried out with grinding resin (GE Healthcare) and electrically-driven disposable pestles (GE Healthcare). Following centrifugation at 14,000g for 5min at 4°C to remove the grinding resin, the supernatant fluid was centrifuged at 100,000g for 1h at 4°C in a Beckman Optima TL ultracentrifuge using a TLS-55 rotor. Supernatant fluid was incorporated into liposomes as described by Davies *et al*. (1990)[10]. Pellets of 1718 cells were similarly extracted. Dissected rat (typically 3 months old) forebrain grey matter was stored at -80°C and allowed to thaw on wet ice in the above solubilisation medium, ratio 0.5g wet weight tissue to 2ml medium. Following homogenisation in a Dounce Tissue Grinder (loose & tight fitting glass pestles were used in succession) and centrifugation at 14,000g for 5min at 4°C, the supernatant fluid was centrifuged at 100,000g for 1h at 4°C as described above. The clear supernatant fluid [14.9 ± 0.5μg protein/μl (s.e.m.)] from the latter centrifugation was used for incorporation into liposomes.

Growth cone collapse assays

These were carried out using whole- or half-DRGs dissected from embryonic day 7 (E7) chick embryos (stage 30-32) or (for retinal axons) from dissected pieces (~50μM diameter) of E7 chick retina. DRG explants were grown for 24h on glass coverslips coated with poly-L-lysine (Sigma-Aldrich) and laminin (Sigma-Aldrich), in the presence of nerve growth factor (NGF, 40ng/ml, Sigma-Aldrich); full details of the assay method used in our laboratory have been published. Retinal explants were grown as for DRGs but without NGF and with medium supplemented with N-2 (Sigma-Aldrich, 100x concentrate) and bovine pituitary extract (200μg/ml, Life Technologies). Cultures were fixed 1h after addition of each treatment, and growth cones were assessed by phase-contrast microscopy. They were classified as either spread or collapsed according to morphological criteria[58]. The validity of this method has been shown when compared to equivalent results using phalloidin staining[59] and

anti-tubulin staining[60]. Results are presented as the mean percentage collapse of growth cones extended from individual DRG explants.

Assessment of PDI inhibitors using collapse assay

Conditions of controls and reagents were assigned randomly to each culture and all experiments were blind-coded. Unless otherwise specified all components were added simultaneously and incubated for 1h (37°C/5% CO_2) before fixation. In experiments with antibody preparations, controls using the same concentration of non-immune rabbit IgG (Sigma-Aldrich G2018, Lot#051K7670), BSA and sodium azide were included. Immunodepletion experiments were performed using Magnetic Dyna Protein A beads (Invitrogen, 70µl packed beads) washed twice in 0.1M phosphate buffer (pH 8) with 0.01% Tween 20 (1ml) by end-over-end mixing for 2.5h at 4°C. Washed beads were added to rat forebrain extracts (RFE) containing either anti-PDI (Sigma-Aldrich P7496 Lot#054K4801), non-immune rabbit IgG or bovine serum albumin (BSA) and mixed end-over-end for 1h at 4°C. Beads were removed on a magnetic separator and the extract subjected to a repeated extraction with fresh beads. Treated extracts were incorporated into liposomes.

Live-staining of csPDI in whole-mounted somite-strips

Stage 22-24 chick embryos were removed from the egg and washed in Leibovitz's L-15 medium (Thermo Fisher Scientific) supplemented with 1% L-Glutamine-Penicillin-Streptomycin solution (Sigma-Aldrich). Embryos were pinned out along the A-P axis, ventral-up, in a Sylgard (Dow Corning) coated dish containing medium. After removal of the endoderm, embryos were re-pinned dorsal-up and the neural tube, intermediate mesoderm and lateral plate mesoderm were separated from the paraxial/somite mesoderm. Strips of somite mesoderm were dissected and collected in 4-chambered cell culture slides (BD Falcon) containing L-15 medium and sheep serum (Sigma-Aldrich, 10% v/v) as blocking solution, and slides incubated for 15min. Primary anti-PDI antibody (Sigma-Aldrich P7496) or rhodamine-conjugated PNA (Vector labs) was added (1:500 v/v) to 3 chambers per slide and incubated for 1h at 38°C. Strips were fixed with 4% formaldehyde for 30min, washed x3 with PBS, 5min per wash, then incubated with secondary antibody (anti-rabbit IgG, Invitrogen) for 2h at 21ºC. Controls for anti-PDI binding, each in the 4th chamber per slide, were: absence of primary antibody, primary antibody pre-absorbed with purified bovine PDI (Sigma-Aldrich, P3818, concentration 5x molarity of anti-PDI antibody), and rabbit IgG (1:500). Slides were mounted with Fluoromount G (SouthernBiotech) and viewed using a Zeiss Axioskop fluorescence microscope. Each staining procedure was repeated at least x3.

Sclerotome and retinal cell staining and transfection

Dissected somite strips were collected in a 2ml LoBind tube (Eppendorf) containing L15 medium, and sclerotome cells were dissociated with a 25G needle, after which 20µl of cells were transferred into each chamber of a 4-chambered cell culture slide (BD Falcon) containing 490µl medium per chamber pre-warmed at 37°C. To maintain sclerotome differentiation a notochord fragment was added to each well. Slides were cultured in a humidified box at 37°C for 16h, after which csPDI was assessed by anti-PDI- and PNA-staining as described above for somite strips. For retinal cells, eyes were removed from stage 22-24 embryos using a microscalpel, and retinal cells dissociated and stained as for sclerotome cells. For siRNA transfection, cells were incubated at 38°C for 16h. 10µl of transfection mix [12.5µg siRNA in 100µl 5% glucose and 1.5µl TurbofectTM (Thermo Fisher Scientific)] in 490µl of DMEM (Sigma-Aldrich) supplemented with B-27 (Life Technologies) and NGF (Sigma-Aldrich) was then added to cultures. After overnight incubation at 38°C cells were washed x3 in DMEM and incubated for 3h with B-27/NGF-supplemented DMEM.

Human astrocytic (1718) cell staining

Human astrocytoma-derived 1718 cells [CCF-STTG1 (ATCC® CRL-1718TM)] were cultured in RPMI 1640 medium (ATCC modification, Gibco) supplemented with 10% fetal bovine serum (FBS; Gibco) and penicillin-streptomycin (Gibco). Cells were maintained at 37°C in 5% CO_2. At each passage, cells were detached using Trypsin-EDTA (0.05%, Gibco), centrifuged at 1000g for 5min and plated in cell culture flasks (Nunc). After removing culture medium, cells were scraped in PBS or diethyl pyrocarbonate (DEPC) PBS and collected in an Eppendorf tube, then centrifuged at 2,000g for 10min at 4°C. Re-suspended cells were washed once with RPMI 1640 and blocked with RPMI 1640/10% goat serum (Sigma-Aldrich) for 10min at room temperature. They were plated in 4-well Millicell EZ slides (Millipore) coated with poly-L-lysine (0.01%, Sigma-Aldrich), at a concentration of 50,000 cells per well (1.7cm2). Cells were incubated with primary antibody in RPMI 1640/1% goat serum for 30min at 4°C, washed x3 with RPMI 1640, then incubated with secondary antibody in RPMI 1640/1% goat serum for 1h at 4°C and washed x3 with RPMI. Cells were fixed with 4% w/v formaldehyde and 15% w/v sucrose in PBS, pH 7.4, for 10min at 21°C, then washed for 5min x3 with PBS. For live-cell imaging of the ER, cells were washed once with HBSS and incubated with ER-TrackerTM Green (BODIPY® FL Glibenclamide, Life Technologies) for 20min at 37°C. Cells were then washed x3 with HBSS and slides were mounted using Fluoromount-G (Southern Biotech). For intracellular immunostaining cells were washed x1 with PBS, fixed with 4% w/v formaldehyde/15% w/v sucrose in PBS for 10min at 21°C, then washed for 5min x3 with PBS. Cells were blocked with PBS with or without 0.1% Triton X-100 (PBS-T) and 10% v/v goat serum for 1h at 21°C. They were then incubated in primary antibody in PBS-T/1% goat serum overnight at 4°C, washed x3 with PBS, incubated for 1h in secondary antibody in PBS-T at room temperature, then washed x3 with PBS. Nuclear staining was performed with 4',6-diamidino-2-phenylindole (DAPI, Sigma-Aldrich) diluted 1:4000 in PBS, or with Hoechst diluted 1:5000 in PBS. Primary antibodies were: rabbit anti-PDI (IgG polyclonal, Sigma-Aldrich) used at 1:250 (live-staining) or 1:500 (post-fixation staining); anti-calnexin (Abcam, clone 6F12BE10, mouse IgG2b) used at 1:100 (live-staining) and 1:200 (post-fixation staining). Secondary antibodies were goat anti-rabbit IgG and goat anti-mouse IgG (Alexa Fluor® 594) used at 1:500.

Embryo fixation and dehydration

Stage 19-22 embryos were washed x2 in PBS before removing the extra-embryonic tissues. Embryos were fixed in 4% w/v formaldehyde for 2h at 21oC, or overnight at 4°C, then rinsed in PBS on a mechanical shaker for 5min and dehydrated through a series of 10min washes x1 with 25, 50, 75% v/v methanol/PBS and 100% methanol. After one further 30min wash in 100% methanol, embryos were stored in methanol at -20°C until required.

Axon staining

After rehydration into PBS-T, embryos were blocked in PBS-T/10% goat serum for 3h at 21oC, then incubated in fluorescein-conjugated PNA (Vector Labs) for sclerotome csPDI, or in anti-tubulin βIII (clone TUJ1, Mouse IgG2a, BioLegend) for axon staining, both at 1:500 in PBS-T/10% v/v goat serum for 12-18h at 4°C. Embryos were then washed x4 for 20min with PBS-T. Secondary antibody (peroxidase goat anti-mouse IgG, Jackson ImmunoResearch) was used at 1:500 in PBS-T/10% goat serum for 2h at 21°C, followed by 20min washes x4 in PBS-T. Embryos were then incubated with 500µg/ml diaminobenzidine (DAB) substrate and 0.006% H_2O_2 in PBS/0.5% Triton, and the colour reaction was developed for 5-10min at 21°C.

Vibratome sectioning

Formaldehyde-fixed embryos were embedded in 10% gelatin (bloom 300, Sigma-Aldrich) in PBS at 38°C for 30min. Cryomolds (Tissue-Tek) with gelatin were set at 21°C for 15min, after which embryos were transferred to them and the gelatin flattened and set at 4C for 30min. Blocks were cut and fixed with 4% formaldehyde at 4ºC for at least 72h, then washed for 10min x3 in PBS, trimmed and mounted in a Leica VT1000 S vibratome. Sections were cut at 70µM using a steel blade and mounted on glass slides (VWR International) using Fluoromount G.

Primary cultures of rat cortical astrocytes

Cortical hemispheres from neonatal rat pups (P1-P3) were isolated and dissected in ice-cold DMEM containing penicillin-streptomycin (Gibco). Care was taken to remove meninges and white matter. Cortices from up to 12 pups were pooled and sub-divided in a Petri dish using a razor blade. The tissue was transferred to a 15ml Falcon tube and spinned briefly, then resuspended in 2ml papain solution [0.75% v/v of papain (25mg/ml, 17U/mg protein, Sigma-Aldrich), 40µg/ml DNase I type IV, 2mM L-Cysteine in DMEM with penicillin-streptomycin] and incubated for 1h at 37°C with occasional resuspension. The enzymatic digestion was quenched by adding 2ml trypsin-inhibitor solution [500ug/ml BSA, 40µg/ml DNase I type IV, 1mg/ml Trypsin inhibitor (Sigma-Aldrich)]. Cells were then dissociated by mechanical resuspension in 1ml ovomucoid solution and collected by centrifugation in a 10ml trypsin-inhibitor solution. They were resuspended in culture medium and plated in poly-D-lysine-coated flasks (cells from 1-1.5 brains in one 75cm2 culture flask). Cells were cultured at 37°C/5% CO2 in DMEM (Gibco) supplemented with 10% FBS (Gibco) and penicillin-streptomycin. After 7-10d culture cells were shaken in an orbital shaker at 350-400rpm (1.9cm orbital radius, MaxQ 4450, ThermoFisher Scientific) at 37°C to obtain a culture of cortical astrocytes. Microglia, neurons and oligodendrocytes were detached after an overnight shaking, and medium was then replaced. Cultures consisted in >90% GFAP-positive cells.

siRNA knockdown of csPDI

The fluorescein-labelled siRNA used to knock down csPDI in the chick embryo was designed according to the sequence of an antisense phosphorothioate (S-oligo; nuclease-resistant oligonucleotide) successfully used by Zai *et al*.[24] to knock down csPDI/PDIA1/P4HB in a human erythroleukemia (HEL) cell line. These authors designed three antisense S-oligos against human PDIA1/P4HB mRNA, and one of these reduced the cell surface expression of P4HB significantly (by 74 ± 9.2% compared to the scrambled S-oligo control). The sequence for the successful oligo was 5′-GCAGCGAGACTCCGAACACGGTA-3′, found in the 3’ UTR of the human PDIA1/P4HB mRNA. This sequence was used to find an appropriate target sequence in the 3’ UTR of chicken PDIA1/P4HB. The sequence used to target chick P4HB was 5’-TCGCCCTCACTTGTCTTTA-3’, and was selected using BLAST NCBI anSfold (Wadsworth Center) to ensure maximum binding. A FITC-labelled control scrambled siRNA with the sequence 5’-GCTCTCTCGTCTATCTACT was designed using InvivoGen siRNA Wizard software http://www.sirnawizard.com/scrambled.php. All sequences were subjected to NCBI BLAST to ensure gene-specificity and to avoid mis-targeting. Rescue experiments used a plasmid encoding a fusion protein of mature human PDIA1 (18-508), tagged at its N-terminus with a bovine pre-pro-trypsinogen signal peptide (bPPTSP) and a FLAG-M1 epitope that is exposed after cleavage of the signal peptide (kind gift of Prof David Ron, Department of Clinical Biochemistry, University of Cambridge)[61].

Primer design

Transcript sequences for selected genes were obtained via the National Center for Biotechnology Information (NCBI) GenBank and Ensembl. Primer pairs for each transcript were designed using the Primer-Blast tool available from the NCBI

(http://www.ncbi.nlm.nih.gov/tools/primer-blast/). Primers were selected according to the following rules: (i) primer length 17-30 base pairs; (ii) CG content 50-60%; (iii) melting temperature 55-80°C; (iv) resulting amplification product 400-1200 base pairs. All potential primers were checked against the G. gallus (taxid:9031) genomic database using the Basic Local Alignment Search Tool (BLAST) from NCBI. The outputs from this last step were used to exclude all primers giving more than one significant region of identity (80% cut-off) against the whole chicken genome, or sharing more than 70% similarity with other genes. Selected primers were synthesized (Sigma-Aldrich) with the T7 promoter primer sequence (TAATACGACTCACTATAGGGAG) appended to the 5' end of the reverse primer, to allow direct generation of digoxigenin-labelled antisense RNA probe by *in vitro* transcription using T7 RNA polymerase.

Polymerase chain reaction (PCR) to prepare template for riboprobe synthesis
cDNA samples (2µl) were pipetted into a 200µl thin-wall centrifuge tube and 36µl of DEPC-treated water, 6µl of primer and 50µl of Reddy Mix PCR Master Mix (AB Gene) was added to each. The contents of the tube were briefly mixed and spun down. Tubes were then placed on a heating block of a hot-lid thermal cycler pre-heated to 95°C. Cycling commenced with an initial 2min denaturation step at 95ºC followed by 34 cycles of 95°C for 25sec, annealing at 50°C for 45sec and elongation at 72ºC for 1min; cycling finished with an extension step of 72ºC for 5min. The PCR product length was checked by agarose gel electrophoresis, and the products stored at -20°C until needed for riboprobe synthesis.

Riboprobe synthesis
20µl in vitro transcription reactions were prepared by adding to a 200µl thin-wall PCR tube in the following order: 9µl DEPC-treated water, 4µl nucleoside triphosphate (NTP) mix (2.5mM ATP, 2.5mM CTP, 2.5mM GTP, 1.67mM UTP, 0.833mM digoxigenin-11-UTP), 2µl T7 transcription buffer (Ambion), 2µl T7 RNA polymerase, 1µl RNase inhibitor (Invitrogen), and 2µl PCR product. The tube contents were mixed by pipetting and briefly spun in a microfuge (≤1000g) to settle them. The tube was further incubated at 37°C in a thermal cycler for 2h, after which 1µl DNase I was added and the tube further incubated in a thermal cycler for 15min at 37°C. To stop the reaction, 1µl of 0.5M EDTA was added and mixed by pipetting, and the tube contents spun down. The probe was then analysed using a Picodrop spectrophotometer.

Isolation of RNA for antisense RNA probes and cDNA synthesis
Embryos were rinsed with cold diethyl pyrocarbonate (DEPC)-PBS and transferred to a methanol-washed Petri dish coated with Sylgard. The extra-embryonic membranes were removed using Watchmaker's forceps pre-cleaned with RNAse Zap (Ambion). Embryos were placed in RNAlater (Ambion) and stored overnight at 4°C. Total RNA was extracted using silica-membrane RNeasy spin columns (Qiagen) according to manufacturer's instructions. cDNA was synthesized using the iScript cDNA synthesis kit (Bio-Rad) according to manufacturer's instructions and stored at -20°C.

Whole-mount in situ hybridization (WMISH)
Our procedure was based on Wilkinson (1998)[62]. Embryos were rehydrated into PBS-T through a series of 75% v/v methanol/ultra-pure water, 50% v/v methanol/ultra-pure water, 25% v/v methanol/PBST. Embryos were transferred into 18-well plates (Nunc). Unless otherwise specified, all reagents were diluted in PBS-T and washes were for 10min in PBS-T on a rocking platform at 21°C. To increase probe permeability embryos were incubated at 21°C in 10µg/ml proteinase K (Roche) for the following durations: embryos to stage 15 for 5min, stage 16-18 for 10min and stage 19-24 for 15min. Embryos were rinsed x1, post-fixed for 20min in 4%

formaldehyde and washed x2 to remove fixative. They were equilibrated with hybridization mix [50% v/v formamide, 5X SSC (Sigma-Aldrich), 2% blocking powder (Boehringer, 1096176), 0.1% Triton X-100, 0.1% CHAPS (Sigma-Aldrich), 1 mg/ml tRNA (Sigma-Aldrich), 5mM EDTA, 50 µg/ml heparin] by rinsing x1 in a 1:1 mixture of PBST/hybridization mix and then x2 in hybridization mix. Plates were then placed at 67°C in a hybridization rocking oven for a minimum pre-hybridization of 2h to 12h maximum, after which the solution was changed to pre-warmed hybridization solution containing 1µg/ml RNA probe, and incubated for at least 12h to 72h maximum. In order to avoid cross contamination, WMISH probes were well separated when the hybridization was being done; vials were leak-proof, and each probe was used no more than x3. After incubation embryos were rinsed x2 and washed x1 with pre-warmed hybridization mix, washed x2 for 30min with hybridization mix, and then x2 with a 1:1 mixture of hybridization mix/PBS-T at 60°C. Embryos were then rinsed x3 with PBS-T. Hybridization solution was eliminated by 30min washes x7 in PBST at 21°C in a rocking shaker. To block non-specific binding, embryos were incubated for 1-3h in blocking solution (10% v/v Sigma-Aldrich sheep serum in PBS-T) at 21°C. This was replaced with blocking solution containing alkaline phosphatase-conjugated anti-digoxigenin Fab fragments (Roche) at 1:2000 dilution, and embryos were incubated further for 12-18h at 4°C. The antibody was removed by rinsing the embryos x3 in PBST with 1mM levamisol, followed by 4h of washes with buffer changes every 30min; in some cases embryos were left overnight at 4°C. Alkaline phosphatase was detected using a mixture of 4-nitro blue tetrazolium chloride (NBT) and 5-bromo-4-chloro-3'-indolyphosphate (BCIP). Embryos were first washed x2 in NTMT (100 mM NaCl, 100 mM Tris-HCl pH 9.5, 50 mM MgCl2, 0.1% Triton X-100), followed by addition of the reaction mixture (4.5 µl/ml NBT and 3.5 µl/ml BCIP in NTMT). Reactions were left in the dark until a deep purple colour had developed; this could take 3h to 5d, and in the latter case the stain solution was replaced daily. Embryos were then washed x3 in PBS-T and fixed in 4% w/v formaldehyde for 12-18h at 4°C. The fixative was removed by several PBS washes. Embryos were imaged using a Leica dissecting microscope and prepared for vibratome sectioning.

siRNA preparation

Lyophilized FITC-labelled RNA duplexes (Dharmacon Thermo Scientific) were obtained in 2' deprotected, annealed and desalted form, dissolved in PCR grade water (Roche) at 3µg/µl and stored in aliquots at -80°C. The transfection solution was 1µg/µl siRNA, 10% polyethylene glycol (PEG) (Carbowax 6000, Union Carbide) and 20% TurbofectTM (Thermo Fisher Scientific, Catalog # R0541). For 2.8µl of siRNA preparation, 1µl of siRNA, 1.2µl of 20% PEG stock and 0.6µl of TurbofectTM were incubated at 21°C for 30min before application. This technique was also tested using pCAβ-EGFPm5[63], a kind gift of Dr. Matthieu Vermeren (Department of Physiology, Development and Neuroscience, University of Cambridge, UK). The final transfection solution contained 2µg/µl plasmid, 10% PEG and 40% TurbofectTM. For a final 5µl of solution, 1µl of plasmid, 2µl of 20% PEG stock and 2µl of TurbofectTM were used; this solution was only used once. For siRNA delivery *in ovo*, borosilicate glass capillaries (WPI, outside diameter 1.5mm, inside diameter 1.12mm) were pulled on a Narishige Puller PC-10 at 62°C. Tips were broken to obtain a suitably narrow internal diameter and capillaries attached to a rubber tube/mouth-pipette.

In ovo transfection

Eggs were cleaned with methanol and 3-4ml of ovalbumin removed using a 19G needle and syringe. The upper side of the egg was reinforced with adhesive tape and a window ~1cm diameter cut through shell and tape using curved scissors. The embryo was raised to the level of the window by re-pipetting the ovalbumin, and visualized by injection into the yolk of ~0.2ml black ink (Pelikan Fount India, 5% in PBS). A small incision was made in the vitelline membrane overlying the posterior

part of the embryo using a microscalpel. The glass capillary containing siRNA/plasmid transfection solution was inserted into the most posterior and newly formed somite of stage 10-14 embryos, and carefully advanced anteriorly within or immediately ventral to the somite mesoderm on one side of the embryo, parallel to the neural tube and dorsal to the endoderm, until the most anterior accessible somite was reached. The capillary was then slowly withdrawn and siRNA was injected into 8-12 successive sclerotomes, each over 5-10 sec (~0.05µl total volume injected per embryo). Care was taken to avoid the upper two cervical segments where the avian spinal accessory nerve exits and ascends immediately adjacent to the neural tube. After pipette withdrawal the embryo was returned to the egg by removing 5ml of ovalbumin, and the window closed with adhesive tape. Each egg was re-incubated for 24h, when siRNA delivery in somites on the injected side was confirmed by the presence of fluorescence in >8 consecutive somites *in ovo* viewed by epifluorescence microscopy. Eggs were then incubated for 24h further to stages 22-24, when embryos were processed for somite strip or sclerotome cell culture and staining, or immunohistochemistry or *in situ* hybridization, all as described above.

Antibodies

Polyclonal rabbit anti-PDI (Sigma-Aldrich P7496) was prepared using PDI purified from bovine liver as immunogen. The whole serum was fractionated and further purified by ion-exchange chromatography to provide the IgG fraction essentially free of other rabbit serum proteins. In this study Lot#054K4801 (protein content 7.1mg/ml in 0.1M phosphate buffered saline pH 7.4 containing 15mM sodium azide) was used. Polyclonal anti-PDI antibody Abcam ab31811 (0.4mg/ml PDI Ab, 1% BSA, 2% Sodium Azide) was raised in rabbit against a synthetic peptide corresponding to human PDI amino acids 400-500 conjugated to keyhole limpet haemocyanin and immunogen affinity-purified; this contained IgG at 0.4mg/ml in 1% BSA, and PBS pH 7.4 containing 0.02% sodium azide as preservative.

PDI inhibitors

Bacitracin (Fluka Lot#13Z3372) was examined for protease activity using azocasein (Sigma-Aldrich Lot#039K7002) as a substrate and protease from Bacillis liceniformis (Sigma-Aldrich Lot#040M1970V) as a standard[33]. A trace (<0.05%) of enzyme was detected and enzyme-free bacitracin reagent was prepared by gel filtration through Sephadex G100[33]. 16F16 (Lot#051M4613V), phenylarsine oxide (Lot#056K1654) and Rutin hydrate (quercetin-3-rutinoside: ≥94%[HPLC] Lot#BCBH6323V) were purchased from Sigma-Aldrich. T3 (3,3',5' triiodo-L-thyonine: Sigma-Aldrich ≥ 95%[HPLC] Lot#016K1628V) was acetylated with acetic acid N-hydroxysuccinimide ester (Apollo Scientific) as described[64] and the product shown to be homogeneous by thin layer chromatography. The propynoic acid carbamoyl methyl amines PACMA31 & PACMA56 were synthesised as described[29].

Other reagents

S-Nitrosoglutathione (Lot#055M403V), L-glutathione reduced (G4251 Lot#SLBH7927V), L-glutathione oxidised (G4626 Lot#100K727625), DL-dithiothreitol (43819, Lot#BCBG3415V) and eosin 5-isothiocyanate (Lot#BCBK9368V) were obtained from Sigma-Aldrich, and L-homocysteine (Lot#B1612) from Santa Cruz Biotechnology. Sema 3A/Fc chimera was from R&D Systems (Lot#1250-53). Agarose bound Peanut Agglutinin (Lot#ZA0611; binding capacity >4.5mg asialofetuin/ml of gel) and Agarose bound Jacalin (Lot#ZA1021) were from Vector Laboratories. Cyanogen bromide-activated Sepharose 4B beads (Sigma C9142) were used to couple purified bovine serum albumin (BSA). After coupling the gel was blocked with 1mM ethanolamine. Beads used in these experiments contained 9.48mg BSA per ml of settled gel.

Protein assay

Protein assays were performed with bicinchoninic acid reagent [Pierce BCA protein assay kit (Lot#QA214075); Sigma Bicinchoninic acid solution (Lot#SHBH4613V) and copper(II) sulphate (Lot#SLBJ6167V) with bovine serum albumin (Pierce Lot#BB42996, 2.0mg/ml in 0.9% NaCl)] as standard, and using the enhanced protocol (60°C for 30min). A separate standard curve was constructed for each assay and the sample was subject to at least 3 separate dilutions which were each determined in duplicate.

Purification of csPDI from somites

A total of 400 chick embryo trunks were fractionated by affinity chromatography on agarose-bound-PNA (Vector Labs), following procedures used previously in the laboratory[10]. Care was taken to elute the affinity column with 0.5M NaCl 1% CHAPS (w/v) and 100mM Tris-HCl (pH7.5), followed by elution with 0.4M lactose/2% CHAPS (w/v) in PBS. Eluates (20µL) were concentrated using StrataClean Resin (Agilent Technologies)[65,66]. Protein bound to the resin was eluted using SDS reducing sample buffer with heating for five minutes at 95°C, followed by centrifugation (10000g for 1min). The supernatant containing the proteins was fractionated on slab gels (7.5% acrylamide separating gel; 5% stacking gel). Samples were examined under reducing conditions and electrophoresis was performed in 25mM Tris (pH 8.3), 192mM glycine, 0.1% SDS. Molecular weight markers (BenchMark Protein Ladder, Invitrogen) were also run. The gel was developed with MS-compatible silver stain using the protocol of Blum *et al*.[67]. The band was excised in a laminar flow hood and submitted for mass spectrometry analysis (Alta Bioscience, UK).

Identifying somite proteins that act as a substrate for S-nitrosylation

The Pierce™ S-Nitrosylation Western Blot Kit (ThermoFisher Scientific) was used, in which a lower background is obtained with iodoTMTzero™ reagent (Lot# PA19543) compared with biotin labelling. A cell free assay was prepared in which 650 somite strips were homogenized in HENS buffer [1ml + 10µl protease inhibitor cocktail (Sigma Lot# 033M4023V)] using an electrically-driven disposable pestle and grinding resin (GE Healthcare). Following centrifugation at 1000g for 1 min at 10°C to remove the resin, the homogenate was centrifuged at 10,000g for 20 min. Aliquots of homogenate containing 200µg protein in 200µl of HENS buffer made 200µM with GSNO. Reduced glutathione was used as a negative control. After incubation at room temperature in the dark for 45min, unreacted GSNO was removed using P6 microcolumns (BioRad) and the samples blocked with methyl methanethiosulfonate. Labelling with iodoTMT reagent was performed in the presence of sodium ascorbate and controls in the presence of water. Protein samples (48µg) were fractionated on NuPAGE 4-12% Bis Tris gels in MOPS buffer and blotted onto Hybond C-extra nitrocellulose membrane using NuPAGE transfer buffer (Thermo Fisher Scientific) containing antioxidant. Blots were probed with anti-TMT antibody (1:1000, Lot#OH190916) purified from mouse ascites fluid with Pierce Goat Anti-Mouse IgG (H+L) HRP conjugate (Lot#OI192080).

Identification of LC1 in somite extracts

An extract of stage 19/20 chick embryo trunks was prepared in HENS buffer containing protease inhibitor (as above for somite strips) and the protein content quantified. An aliquot containing 25µg protein was fractionated on a 4-12% Bis-Tris gel and blotted onto Hybond C-extra nitrocellulose membrane using NuPAGE transfer buffer (Thermo Fisher Scientific) containing antioxidant. The blot was cut in half just above the 41K marker and the top half of the membrane was probed with rabbit anti-tubulin (Sigma, Lot#50K4813) followed by goat anti-rabbit IgG (HRP, Abcam Lot#GR3231028-7, 1:20,000). The bottom half was probed with MAP-1B (LC1) mouse monoclonal antibody against amino acids 2257-2357 of MAP-1B of

mouse origin (Santa Cruz Biotechnology, Inc., sc-136472) followed by goat anti-mouse IgG (HRP, Pierce Lot#TE262980, 1:20,000). Blots were blocked in 5% non-fat dried milk (BioRad) in TBST and thoroughly washed x5, each for 5 min, in TBST. In both above experiments blots were treated with Millipore Immobilon Western Reagent (Lot#1710401) and exposed to film.

Action of D-NAME and L-NAME on S-nitrosylation of LC1

Somite extract (200µg protein for each condition) was incubated at 37°C for 1h in the presence of 300µM D-NAME (Sigma, Lot#BCBM7105V) or L-NAME (Sigma, Lot#BCBT1028). A control experiment with somite extract and buffer alone was included. Subsequently extracts were made 200µM in S-nitrosoglutathione and left at room temperature for 45 min before being processed as above and subjected to fractionation on a Nu-PAGE 4-12% Bis-Tris gel in MOPS buffer followed by blotting on Hybond C-extra. Care was taken to load equal amounts of protein (15µg per lane). Processed samples were assayed for protein levels with a Qubit Fluorometer 2.0 (Thermo Fisher Scientific) using the Qubit protein assay (quantitation range 0.25-5µg) to achieve the same quantity of sample in each lane. The blot was cut in half below the 53K molecular weight marker and the top half probed with rabbit anti-tubulin (Sigma, Lot#50K4813, 1:20,000) and goat anti-rabbit IgG (HRP, Abcam Lot#GR3231028-7) followed by Millipore Immobilon Western Reagent. The damp membrane was examined using an iBright FL1500 imaging system (Thermo Fisher Scientific) and the digital image caught directly by the instrument to authenticate that somite extract was loaded in every lane. The bottom half of the blot was probed with anti-iodoTMT (Lot#PH204668, 1:1000) and goat anti-mouse IgG (H+L) HRP, 1:20,000, followed by Clarity Western ECL substrate (mid-femtogram-level sensitivity, BioRad). The damp membrane was examined in the iBright FL1500 imaging system and the digital image captured.

Western blot of rat cortical astrocyte cell surface proteins

Two month-old wild-type rats (Rattus norvegicus) were used as a source of neonatal rat cerebral cortical astrocytes. Four flasks of cortical astrocytes (in DMEM with 10% FBS and penicillin/streptomycin) at 95% confluence were subjected to biotinylation using a commercial 'Cell Surface Protein Isolation Kit' (ThermoScientific, Prod#89881, Lot#RD234938). Following labelling of the cell surface proteins with NMS-SS-Biotin reagent, the biotinylated proteins were captured on NeutrAvidin resin, washed thoroughly and the bound proteins released by cleavage of the S-S bond by treatment with freshly prepared SDS-PAGE sample buffer made 50mM with respect to DTT. One-third of this eluate was fractionated by SDS-PAGE on a 7.5% polyacrylamide resolving gel (120x80mmx3mm; 5% stacking gel) and blotted onto Hybond C-extra nitrocellulose membrane (Amersham Biosciences Batch No. 319063) using 25mM Tris (pH8.3), 192mM glycine and 0.1% SDS electrophoresis buffer. The blot was blocked with 5% Blotting Grade Non Fat Dry Milk (BioRad) and developed with 1:20,000 anti-PDI (Sigma P7496) followed by 1:2000 Tidy Blot Western Blot Detection Reagent-HRP (BioRad, Batch#160129) and the use of Immobilon Western Chemiluminescent HRP substrate (Millipore).

Assessment of reductase activity in purified PDI

Di-E-GSSG was prepared by the reaction of eosin isothiocyanate (Sigma-Aldrich) with L-glutathione oxidised (Sigma-Aldrich Lot#100K72765) as described in detail by Raturi & Mutus[23]. Four samples of PDI (4µg) were incubated in 20µl 100 mM potassium phosphate (pH7), made 1.5µM with respect to calcium and magnesium chloride, with 20µl packed PNA-agarose beads (Vector lot ZC0504) with a capacity to bind >90µg asialofetuin to 20µl beads. The beads were kept at 5°C over 18h with intermittent mixing. Following centrifugation at 14,000g for 5min at 4°C and a further wash with 30µl of buffer, the combined supernatant fluids were added to the reaction

mixture to give a maximum concentration 128nM PDI. Reductase activity was monitored as above[23]. Fluorescence was measured in a Biotronix Fluorometer (Electronics and Instrumentation Services for Biological Science, University of Cambridge).

Statistics

A non-parametric Kruskal-Wallis one-way ANOVA was used for comparison of data sets. The Mann-Whitney U test was used for comparison between treatment conditions in collapse assays. For comparison between three or more data points a two-way ANOVA was performed, followed by a post-hoc Bonferroni correction. No statistical methods were used to predetermine sample size. Graphs and figures were produced with GraphPad Prism 7.0 and Adobe Photoshop CS6. Histograms show mean +/- s.e.m.

Acknowledgements

We thank C. Stern, M.Bate, C.Holt, R.B.Heap and O.Paulsen for comments on the manuscript. The initial parts of this work were supported by grants from the Medical Research Council and the Wellcome Trust, and more recently by the Rosetrees Trust. J.S. was also supported by a studentship from the International Spinal Research Trust.

Author contributions

G.M.W.C. and R.J.K. designed the experiments, analysed data and wrote the paper; G.M.W.C. also purified and synthesised some of the reagents, and R.J.K. carried out collapse assays and dissected embryo and brain material. C.S. and C.C. performed immunohistochemical and lectin staining of somites. C.S. and E.W. carried out *in ovo* injection experiments. J.S. performed live-staining and collapse assay experiments using astrocytic cells. K.W., P.J., S.P., N.S., A.H., A.A. and S.W. performed collapse assay experiments. G.M.W.C. and A.K. carried out biochemical experiments. G.R.-V. and P.C. performed *in ovo* bead implants. C.S. and R.J.K. carried out siRNA rescue experiments and M.R. assisted with design of the figures and statistics. All authors reviewed the manuscript.

References

1. Keynes, R. J. & Stern, C. D. Segmentation in the vertebrate nervous system. *Nature* **310**, 786-789 (1984).
2. Rickmann, M., Fawcett, J. W. & Keynes, R. J. The migration of neural crest cells and the growth of motor axons through the rostral half of the chick somite. *J Embryol Exp Morphol* **90**, 437-455 (1985).
3. Bronner-Fraser, M. Analysis of the early stages of trunk neural crest migration in avian embryos using monoclonal antibody HNK-1. *Dev Biol* **115**, 44-55 (1986).
4. Fleming, A., Kishida, M. G., Kimmel, C. B. & Keynes, R. J. Building the backbone: the development and evolution of vertebral patterning. *Development* **142**, 1733-1744 (2015).
5. Gammill, L. S., Gonzalez, C., Gu, C. & Bronner-Fraser, M. Guidance of trunk neural crest migration requires neuropilin 2/semaphorin 3F signaling. *Development* **133**, 99-106 (2006).
6. Wang, H. U. & Anderson, D. J. Eph family transmembrane ligands can mediate repulsive guidance of trunk neural crest migration and motor axon outgrowth. *Neuron* **18**, 383-396 (1997).
7. Krull, C. E. et al. Interactions of Eph-related receptors and ligands confer rostrocaudal pattern to trunk neural crest migration. *Curr Biol* **7**, 571-580 (1997).
8. Koblar, S. A. et al. Spinal motor axons and neural crest cells use different molecular guides for segmental migration through the rostral half-somite. *J Neurobiol* **42**, 437-447 (2000).
9. Schwarz, Q., Maden, C. H., Davidson, K. & Ruhrberg, C. Neuropilin-mediated neural crest cell guidance is essential to organise sensory neurons into segmented dorsal root ganglia. *Development* **136**, 1785-1789 (2009).
10. Davies, J. A., Cook, G. M., Stern, C. D. & Keynes, R. J. Isolation from chick somites of a glycoprotein fraction that causes collapse of dorsal root ganglion growth cones. *Neuron* **4**, 11-20 (1990).
11. Keynes, R. et al. Surround repulsion of spinal sensory axons in higher vertebrate embryos. *Neuron* **18**, 889-897 (1997).
12. Kapfhammer, J. P. & Raper, J. A. Collapse of growth cone structure on contact with specific neurites in culture. *J Neurosci* **7**, 201-212 (1987).
13. Raper, J. A. & Kapfhammer, J. P. The enrichment of a neuronal growth cone collapsing activity from embryonic chick brain. *Neuron* **4**, 21-29 (1990).
14. Stern, C. D., Sisodiya, S. M. & Keynes, R. J. Interactions between neurites and somite cells: inhibition and stimulation of nerve growth in the chick embryo. *J Embryol Exp Morphol* **91**, 209-226 (1986).
15. Kozlov, G., Määttänen, P., Thomas, D. Y. & Gehring, K. A structural overview of the PDI family of proteins. *FEBS J* **277**, 3924-3936 (2010).
16. Goldberger, R. F., Epstein, C. J. & Anfinsen, C. B. Acceleration of reactivation of reduced bovine pancreatic ribonuclease by a microsomal system from rat liver. *J Biol Chem* **238**, 628-635 (1963).
17. Ali Khan, H. & Mutus, B. Protein disulfide isomerase a multifunctional protein with multiple physiological roles. *Front Chem* **2**, 70 (2014).
18. Parakh, S. & Atkin, J. D. Novel roles for protein disulphide isomerase in disease states: a double edged sword. *Front Cell Dev Biol* **3**, 30 (2015).
19. Hausman, R. E. & Moscona, A. A. Purification and characterization of the retina-specific cell-aggregating factor. *Proc Natl Acad Sci U S A* **72**, 916-920 (1975).
20. Pariser, H. P., Zhang, J. & Hausman, R. E. The cell adhesion molecule retina cognin is a cell surface protein disulfide isomerase that uses disulfide exchange activity to modulate cell adhesion. *Exp Cell Res* **258**, 42-52 (2000).

21. Bi, S., Hong, P. W., Lee, B. & Baum, L. G. Galectin-9 binding to cell surface protein disulfide isomerase regulates the redox environment to enhance T-cell migration and HIV entry. *Proc Natl Acad Sci U S A* **108**, 10650-10655 (2011).
22. Schaefer, K. et al. Galectin-9 binds to O-glycans on protein disulfide isomerase. *Glycobiology* **27**, 878-887 (2017).
23. Raturi, A. & Mutus, B. Characterization of redox state and reductase activity of protein disulfide isomerase under different redox environments using a sensitive fluorescent assay. *Free Radic Biol Med* **43**, 62-70 (2007).
24. Zai, A., Rudd, M. A., Scribner, A. W. & Loscalzo, J. Cell-surface protein disulfide isomerase catalyzes transnitrosation and regulates intracellular transfer of nitric oxide. *J Clin Invest* **103**, 393-399 (1999).
25. Sobierajska, K. et al. Protein disulfide isomerase directly interacts with β-actin Cys374 and regulates cytoskeleton reorganization. *J Biol Chem* **289**, 5758-5773 (2014).
26. Janiszewski, M. et al. Regulation of NAD(P)H oxidase by associated protein disulfide isomerase in vascular smooth muscle cells. *J Biol Chem* **280**, 40813-40819 (2005).
27. Hamburger, V. & Hamilton, H. L. A series of normal stages in the development of the chick embryo. *J Morphol* **88**, 49-92 (1951).
28. Everson, W. V. & Kao, W. W.-Y. in *Prolyl hydroxylase, protein disulfide isomerase and other structurally related proteins* (ed Guzman, N. A.) 109-126 (CRC Press, New York, 1997).
29. Xu, S. et al. Discovery of an orally active small-molecule irreversible inhibitor of protein disulfide isomerase for ovarian cancer treatment. *Proc Natl Acad Sci U S A* **109**, 16348-16353 (2012).
30. Hess, D. T., Patterson, S. I., Smith, D. S. & Skene, J. H. Neuronal growth cone collapse and inhibition of protein fatty acylation by nitric oxide. *Nature* **366**, 562-565 (1993).
31. Bayir, H. et al. Increased S-nitrosothiols and S-nitrosoalbumin in cerebrospinal fluid after severe traumatic brain injury in infants and children: indirect association with intracranial pressure. *J Cereb Blood Flow Metab* **23**, 51-61 (2003).
32. Massy, Z. A. et al. Increased plasma S-nitrosothiol levels in chronic haemodialysis patients. *Nephrol Dial Transplant* **18**, 153-157 (2003).
33. Rogelj, S., Reiter, K. J., Kesner, L., Li, M. & Essex, D. Enzyme destruction by a protease contaminant in bacitracin. *Biochem Biophys Res Commun* **273**, 829-832 (2000).
34. Bennett, T. A., Edwards, B. S., Sklar, L. A. & Rogelj, S. Sulfhydryl regulation of L-selectin shedding: phenylarsine oxide promotes activation-independent L-selectin shedding from leukocytes. *J Immunol* **164**, 4120-4129 (2000).
35. Primm, T. P. & Gilbert, H. F. Hormone binding by protein disulfide isomerase, a high capacity hormone reservoir of the endoplasmic reticulum. *J Biol Chem* **276**, 281-286 (2001).
36. Hoffstrom, B. G. et al. Inhibitors of protein disulfide isomerase suppress apoptosis induced by misfolded proteins. *Nat Chem Biol* **6**, 900-906 (2010).
37. Sliskovic, I., Raturi, A. & Mutus, B. Characterization of the S-denitrosation activity of protein disulfide isomerase. *J Biol Chem* **280**, 8733-8741 (2005).
38. Owen, J. B. & Butterfield, D. A. in *Protein Misfolding and Cellular Stress in Disease and Aging: Concepts and Protocols* (eds Bross, P. & Gregersen, N.) 269-277 (Springer Science & Business Media, 2010).
39. Ascenzi, P. & Brunori, M. Myoglobin: a pseudo-enzymatic scavenger of nitric oxide. *Biochemistry and Molecular Biology Education* **29**, 183-185 (2001).
40. Rayner, B. S., Hua, S., Sabaretnam, T. & Witting, P. K. Nitric oxide stimulates myoglobin gene and protein expression in vascular smooth muscle. *Biochem J* **423**, 169-177 (2009).

41. Stroissnigg, H. et al. S-nitrosylation of microtubule-associated protein 1B mediates nitric-oxide-induced axon retraction. *Nat Cell Biol* **9**, 1035-1045 (2007).
42. Keynes, R. J., Johnson, A. R., Picart, C. J., Dunin-Borkowski, O. M. & Cook, G. M. A growth cone collapsing activity in chicken gray matter. *Ann N Y Acad Sci* **633**, 562 (1991).
43. Ghosh, A. & David, S. Neurite growth-inhibitory activity in the adult rat cerebral cortical gray matter. *J Neurobiol* **32**, 671-683 (1997).
44. Jasuja, R. et al. Protein disulfide isomerase inhibitors constitute a new class of antithrombotic agents. *J Clin Invest* **122**, 2104-2113 (2012).
45. Akiyama, H., Chaboissier, M. C., Martin, J. F., Schedl, A. & de Crombrugghe, B. The transcription factor Sox9 has essential roles in successive steps of the chondrocyte differentiation pathway and is required for expression of Sox5 and Sox6. *Genes Dev* **16**, 2813-2828 (2002).
46. Stolt, C. C. et al. The Sox9 transcription factor determines glial fate choice in the developing spinal cord. *Genes Dev* **17**, 1677-1689 (2003).
47. Sun, W. et al. SOX9 Is an astrocyte-specific nuclear marker in the adult brain outside the neurogenic regions. *J Neurosci* **37**, 4493-4507 (2017).
48. Vermeren, M. M., Cook, G. M., Johnson, A. R., Keynes, R. J. & Tannahill, D. Spinal nerve segmentation in the chick embryo: analysis of distinct axon-repulsive systems. *Dev Biol* **225**, 241-252 (2000).
49. Steketee, M. B. & Tosney, K. W. Contact with isolated sclerotome cells steers sensory growth cones by altering distinct elements of extension. *J Neurosci* **19**, 3495-3506 (1999).
50. Huber, A. B. et al. Distinct roles for secreted semaphorin signaling in spinal motor axon guidance. *Neuron* **48**, 949-964 (2005).
51. Ramachandran, N., Root, P., Jiang, X. M., Hogg, P. J. & Mutus, B. Mechanism of transfer of NO from extracellular S-nitrosothiols into the cytosol by cell-surface protein disulfide isomerase. *Proc Natl Acad Sci U S A* **98**, 9539-9544 (2001).
52. Shah, C. M., Bell, S. E., Locke, I. C., Chowdrey, H. S. & Gordge, M. P. Interactions between cell surface protein disulphide isomerase and S-nitrosoglutathione during nitric oxide delivery. *Nitric Oxide* **16**, 135-142 (2007).
53. Flögel, U., Merx, M. W., Godecke, A., Decking, U. K. & Schrader, J. Myoglobin: A scavenger of bioactive NO. *Proc Natl Acad Sci U S A* **98**, 735-740 (2001).
54. Cox, E. C., Müller, B. & Bonhoeffer, F. Axonal guidance in the chick visual system: posterior tectal membranes induce collapse of growth cones from the temporal retina. *Neuron* **4**, 31-37 (1990).
55. Goplen, D. et al. Protein disulfide isomerase expression is related to the invasive properties of malignant glioma. *Cancer Res* **66**, 9895-9902 (2006).
56. Loh, K. H. et al. Proteomic analysis of unbounded cellular compartments: synaptic clefts. *Cell* **166**, 1295-1307.e21 (2016).
57. Xiao, G., Chung, T. F., Pyun, H. Y., Fine, R. E. & Johnson, R. J. KDEL proteins are found on the surface of NG108-15 cells. *Brain Res Mol Brain Res* **72**, 121-128 (1999).
58. Cook, G. M., Jareonsettasin, P. & Keynes, R. J. Growth cone collapse assay. *Methods Mol Biol* **1162**, 73-83 (2014).
59. Manns, R. P., Cook, G. M., Holt, C. E. & Keynes, R. J. Differing semaphorin 3A concentrations trigger distinct signaling mechanisms in growth cone collapse. *J Neurosci* **32**, 8554-8559 (2012).
60. He, Y., Yu, W. & Baas, P. W. Microtubule reconfiguration during axonal retraction induced by nitric oxide. *J Neurosci* **22**, 5982-5991 (2002).
61. Zito, E. et al. Oxidative protein folding by an endoplasmic reticulum-localized peroxiredoxin. *Mol Cell* **40**, 787-797 (2010).

62. Wilkinson, D. G. *In Situ Hybridization: A Practical Approach* (Oxford University Press, Oxford, 1998).
63. Bron, R. et al. Boundary cap cells constrain spinal motor neuron somal migration at motor exit points by a semaphorin-plexin mechanism. *Neural Dev* **2**, 21 (2007).
64. Gallina, A. et al. Inhibitors of protein-disulfide isomerase prevent cleavage of disulfide bonds in receptor-bound glycoprotein 120 and prevent HIV-1 entry. *J Biol Chem* **277**, 50579-50588 (2002).
65. Bonn, F. et al. Picking vanished proteins from the void: how to collect and ship/share extremely dilute proteins in a reproducible and highly efficient manner. *Anal Chem* **86**, 7421-7427 (2014).
66. Otto, A., Maaß, S., Bonn, F., Büttner, K. & Becher, D. An Easy and Fast Protocol for Affinity Bead-Based Protein Enrichment and Storage of Proteome Samples. *Methods Enzymol* **585**, 1-13 (2017).
67. Blum, H., Beier, H. & Gross, H. J. Improved silver staining of plant proteins, RNA and DNA in polyacrylamide gels. *Electrophoresis* **8**, 93-99 (1987).
68. Carmichael, D. F., Morin, J. E. & Dixon, J. E. Purification and characterization of a thiol:protein disulfide oxidoreductase from bovine liver. *J Biol Chem* **252**, 7163-7167 (1977).

Figures and Figure Legends

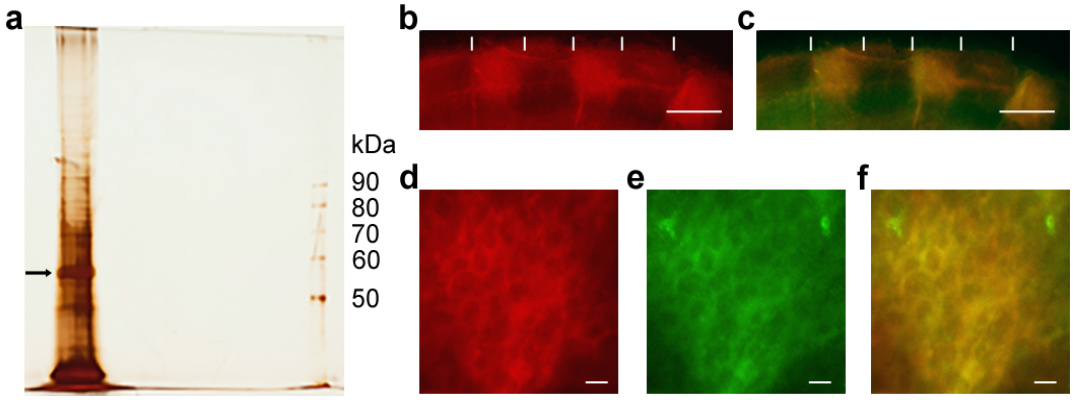

Figure 1

Identification of csPDI in somites

a, Silver-stained SDS-PAGE of lactose eluate of chick somite proteins bound to PNA-agarose; arrow indicates the major band of 57kDa.

b, c, Somite strip live-stained with rhodamine-PNA (red, b) and co-stained with fluorescein-conjugated anti-PDI; preferential staining of three P-half-sclerotomes is shown; PNA staining and anti-PDI staining are co-localized (yellow, c); vertical white lines indicate half-somite boundaries; Scale bars 50μM.

d-f, Higher magnification of b and c showing ring staining at the cell periphery by rhodamine-PNA (d) and by fluorescein-conjugated anti-PDI (e), and their co-localisation (yellow, f). Scale bars 5μM.

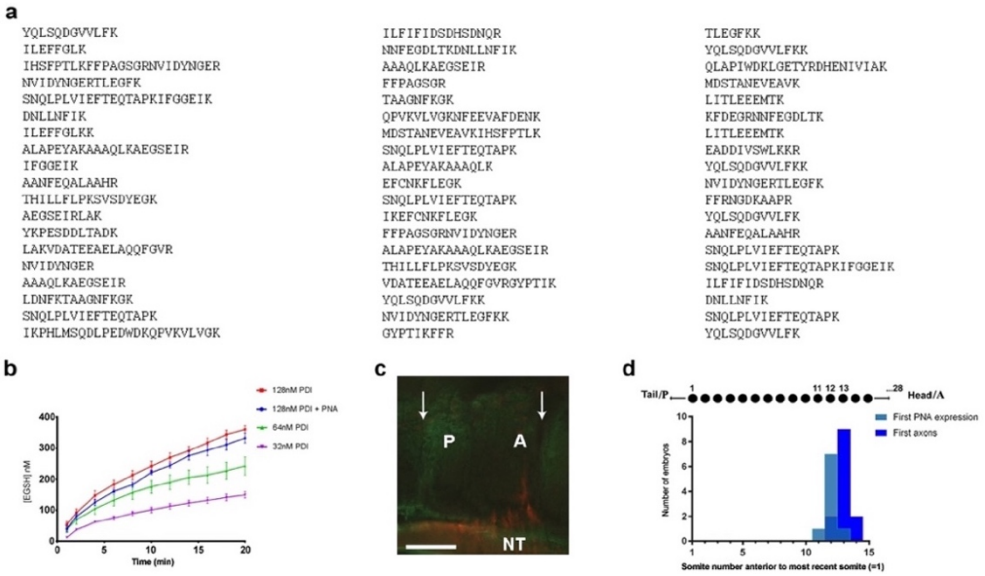

Figure 1-figure supplement 1

Identification of csPDI in somites

a, Identification of csPDI in somites by mass spectrometry. The major band seen in Fig. 1a (arrow) was carefully excised and dispatched to Alta Bioscience (UK) for tryptic digestion and examination by mass spectrometry. The 57-peptide tryptic digest amino acid sequences correspond to chicken PDI, subtype PDIA1 or P4HB.

b, Reductase activity in purified PDI. Three concentrations of purified PDI (Sigma-Aldrich; 128nM, 64nM, 32nM) were examined for reductase activity using dieosin glutathione disulphide (Di-E-GSSG). Two-way analysis of variance and multiple comparisons using the Bonferroni test showed no significant difference between the upper curves (blue and red). This is in accord with the carbohydrate composition of this enzyme preparation. Bovine liver PDI is a glycoprotein with 12% by weight of carbohydrate; L-fucose and N-acetylgalactosamine are not present in detectable quantities[68]. The lack of the latter sugar indicates that O-glycosylation is not a feature of this liver enzyme.

c, Onset of csPDI expression in somites. A parasagittal section (10μM) showing a somite with its A- and P-halves flanked on each side by adjacent half-somites, stained for csPDI using fluorescein-conjugated PNA (green), and for the first emerging spinal axons (red) using TUJ1 antibody; arrows indicate the somite boundaries; axons emerge from the neural tube in the A-half of the somite (A), and PNA-staining is visible in the P-half (P). NT, neural tube. Scale bar 40μM.

d, Onset of csPDI expression in 11 stage 16/17 chick embryos (26-32 somites), assessed using 10μM parasagittal sections of somites stained with fluorescein-conjugated PNA; the X-axis and upper schematic diagram show the somite positions (11, 12, 13) where PNA-staining was first detected in individual embryos, counting somites in a P-A (left-right) direction (most recently formed somite = 1). The first emerging spinal axons (stained using TUJ1 antibody) either coincided with the onset of PNA staining (1/11 embryos), or were delayed by the time taken to form one more somite (9/11 embryos) or two more somites (1/11 embryos). Since each somite takes ~90min to form, csPDI expression precedes axon outgrowth in each segment by ~90-180min.

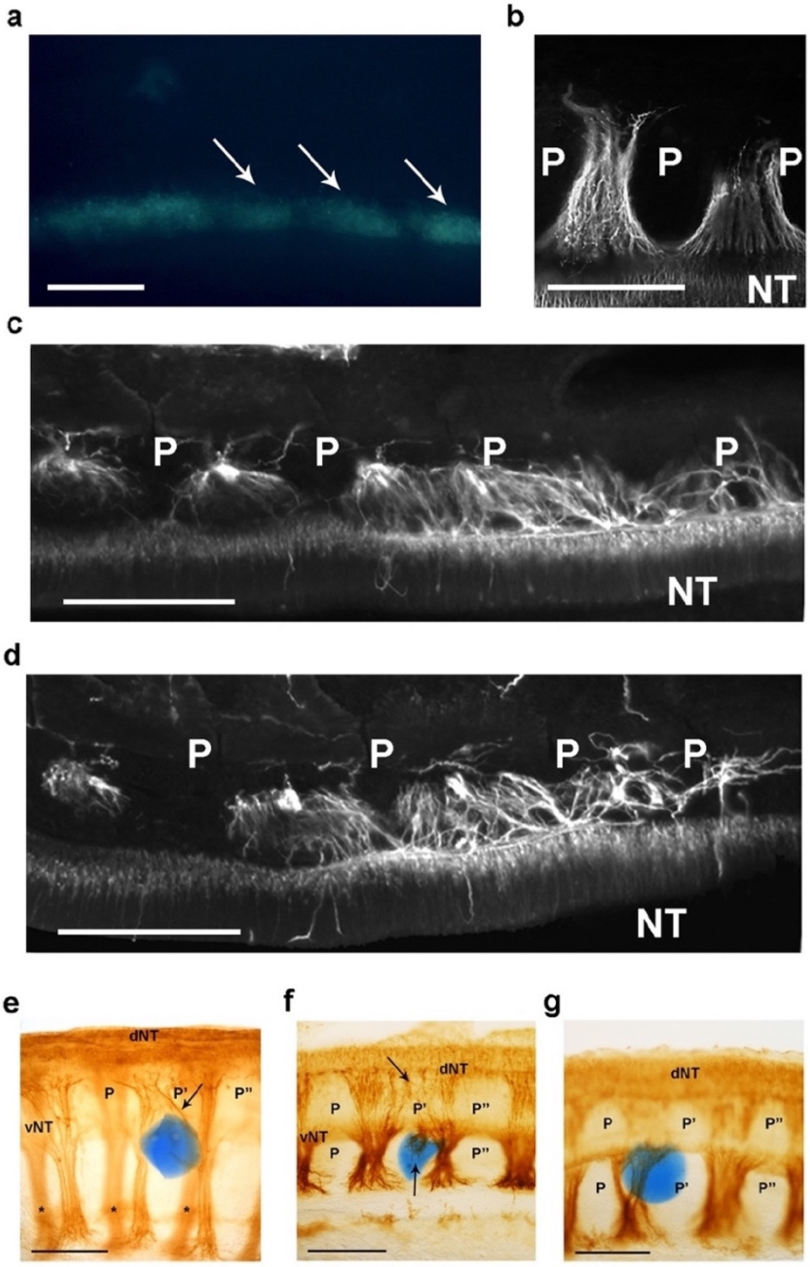

Figure 2

csPDI mediates nerve patterning in vivo

a, Image of a live embryo *in ovo*, viewed from above, taken 24 hours after injection of fluorescein-labelled siRNA into somites (arrows) on one side; label is distributed throughout the A- and P-half-sclerotomes of each somite, and is visibly diminished at 3 consecutive somite boundaries. Scale bar 100μM.

b, Representative image of normal motor axon segmentation following scrambled siRNA delivery. Longitudinal section stained using fluorescein-conjugated TUJ1 antibody. Scale bar 100μM.

c, d, Loss of axon segmentation in two embryos after PDI siRNA knockdown. The siRNA-treated side of each embryo is shown; axons are segmented normally (left) but segmentation is absent (right) where axons grow into P-half-sclerotomes (P). NT, neural tube. Scale bars 100μM.

e, f, Loss of axon segmentation in embryos after *in ovo* implantation of PACMA 31-impregnated bead (blue); embryos were stained using HRP-labelled TUJ1 antibody and viewed as whole-mounts (e) or as implanted-side-only half-mounts (f); abnormal

growth of sensory axons (arrow, e; upper arrow, f) towards dorsal neural tube (dNT) in P-half-sclerotome (P'), compared with normal projections avoiding two adjacent P-half-sclerotomes (P, P''); lower arrow (f) indicates motor axons sprouting from ventral neural tube (vNT) into P-half-sclerotome; asterisks, spinal axons on opposite side of whole-mount (e). Scale bars 150μM.
g, Normal segmentation of dorsal/sensory axons and ventral/motor axons after implantation of PACMA 56 bead; P, P', P'', dorsal and ventral domains of 3 consecutive P-half-sclerotomes. Scale bar 150μM.

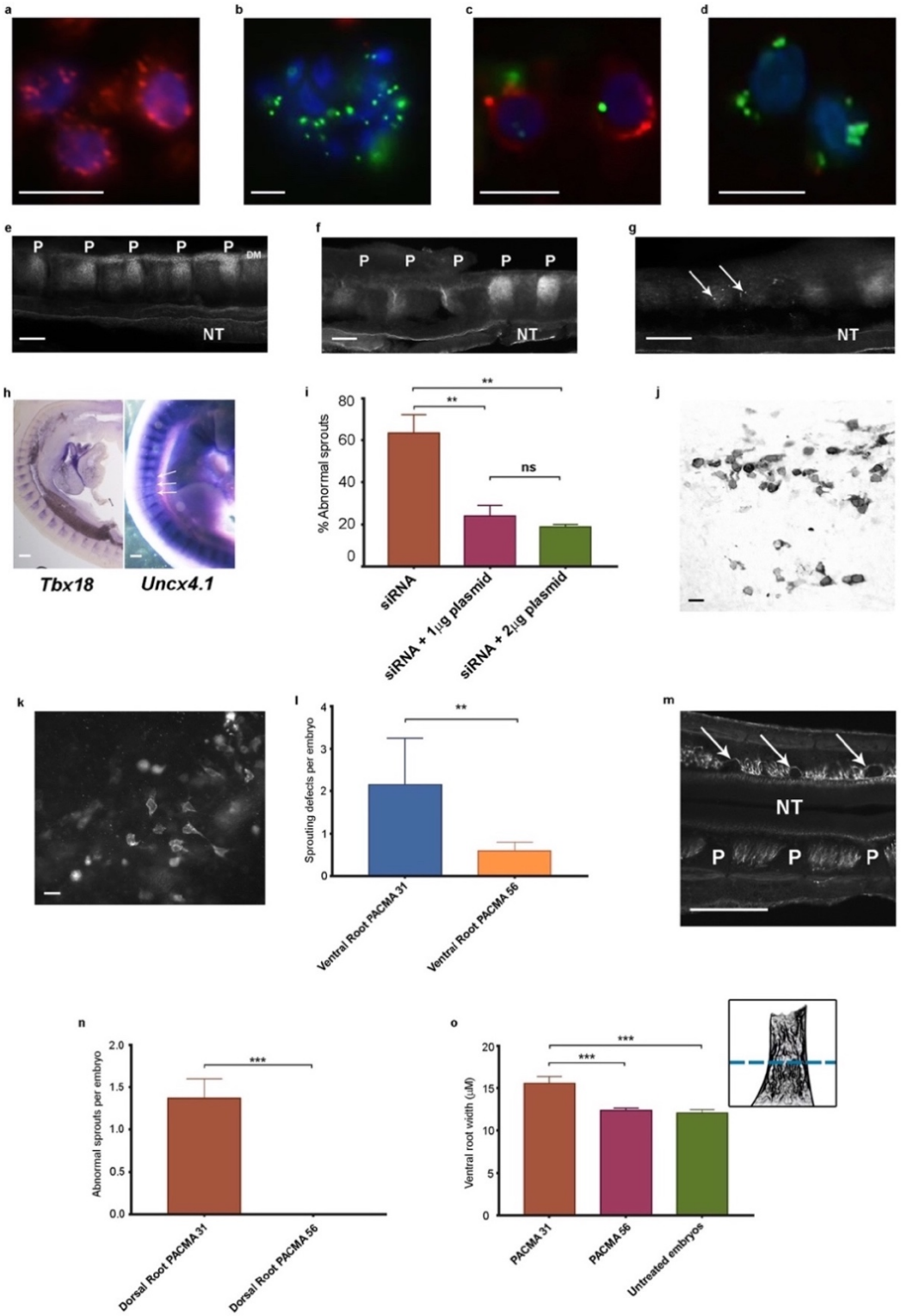

Figure 2-figure supplement 2

a, Chick retinal cells after transfection with scrambled siRNA, stained with anti-PDI antibody (red) and the nuclear marker DAPI (blue). Scale bar 10μM.

b, Stained as in a, after PDI knockdown using FITC-siRNA (green). Scale bar 10μM.

c, d, P-half-sclerotome cells showing PDI expression (red) after transfection with scrambled FITC-siRNA (green) (c), and loss of PDI expression after knockdown with FITC-siRNA (green; d). Scale bar 10μM.

e, Somite strip after injection of control scrambled siRNA, showing normal PNA expression in 5 P-half-sclerotomes along the A-P axis. P-half-sclerotome, P; Dermomyotome, DM; neural tube, NT. Scale bar 50μM.
f, g, Somite strips stained for PNA after siRNA PDI knockdown. f, loss of PNA staining in three P-half-somites (left) compared with two normally stained P-half-somites (right); P, P-half-sclerotome; g, loss of PNA staining in two segments with residual spots of FITC-siRNA expression (arrows). Scale bars 50μM.
h, Left, sagittal section of a stage 22 siRNA-transfected embryo, hybridized with a *Tbx18* probe; regional expression in A-half-somites is unaltered. Scale bar 100μM. Right, stage 22 PDI-siRNA transfected whole-mounted embryo, hybridized with an *Uncx4.1* probe, showing diminished expression in 3 P-half-sclerotomes (arrows). Scale bar 100μM.
i, Rescue of siRNA-induced ventral root/motor axon phenotype by co-injection *in ovo* of siRNA with PDI-expressing plasmid (1μg or 2μg as indicated). For each histogram bar, 10 consecutive somites in the injected region of each embryo were assessed (blind-coded) for the presence or absence of motor axons projecting abnormally into P-half-somite, using anti-TUJ1-stained whole-mounted embryos.
j, Sclerotome cells stained with HRP-labelled anti-PDI antibody in a whole-mounted embryo that received co-injected siRNA and plasmid (1μg). Scale bar 5μM.
k, Sclerotome cells stained with fluorescein-conjugated anti-FLAG-M1 antibody in a whole-mounted embryo that received co-injected siRNA and plasmid (1μg). Scale bar 5μM.
l, PACMA 31 (200μM administered by direct injection to somites on one side *in ovo*) caused a significant increase in aberrant motor/ventral root axon sprouting compared with PACMA 56 injection.
m, PACMA 31 (200μM by direct injection *in ovo*) resulted in dorsal 'bridges' of sensory axons (arrows) interconnecting adjacent axon bundles, contrasting with the normal dorsal/sensory axon segmentation on the non-injected side (NT, neural tube; P, P-half-sclerotome). Scale bar 100μM.
n, PACMA 31 (200μM by direct injection *in ovo*) showing the incidence of dorsal bridges of sensory axons in PACMA 31-injected embryos compared with their absence in PACMA 56-injected embryos (P56).
o, Assessment of ventral root A-P width after PACMA injection (200μM) into somites *in ovo*. Sections of stage-21 TUJ1-stained embryos were blind-coded and assessed by fluorescence microscopy. Images were taken with QCapture Pro 6.0 and analyzed with ImageJ, measuring the A-P width of the ventral root at the most proximal position where constituent motor axons align in parallel (schematic inset upper right, above dashed line); n=12 embryos (PACMA31), n=9 embryos (PACMA56), n=10 embryos (untreated).

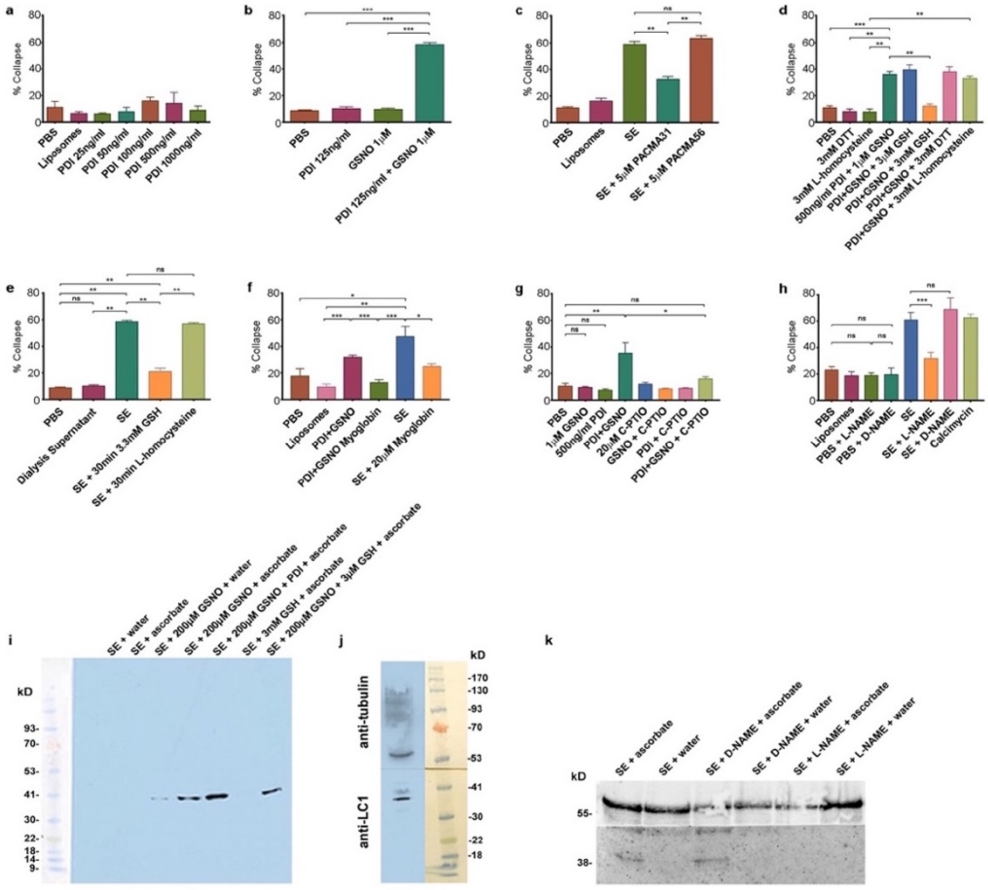

Figure 3

csPDI mediates axon repulsion in vitro

a, Collapse assays testing purified bovine PDI in liposomes at a range of concentrations; controls, phosphate-buffered saline (PBS) and untreated liposomes; histogram shows mean +s.e.m.

b, Assays testing PDI and GSNO applied individually or concomitantly.

c, Assays testing PACMA31 and PACMA56 on somite extracts (SE).

d, Assays testing reducing agents at the concentrations indicated when applied either alone or together with PDI+GSNO.

e, Assays testing GSH and L-homocysteine on SE-induced collapse.

f, Assays testing myoglobin (20μM) on SE- and PDI+GSNO-induced collapse.

g, Assays testing carboxy (C)-PTIO (20μM) on PDI+GSNO-induced collapse.

h, Assays testing L-NAME and its control D-NAME on SE-induced collapse; calcimycin was used as a positive control.

i, S-nitrosylated protein (iodo-TMT-labelled) in somites; protein samples (48μg) from somite cell-free extracts were fractionated on NuPAGE 4-12% Bis Tris gels as described in the Methods; lanes 1 & 2 are controls consisting of somite proteins only, with no detectable signal compared with lanes 3 & 4 where GSNO has been added; lane 3 is a control (treated with water) showing negligible iodoTMT labelling, and lane 4 (reduced with ascorbate to generate a new free thiol for labelling) shows increased label; lane 5 shows that addition of PDI (1μg/0.1ml reaction mixture) enhances labelling; lane 6 shows that 3mM GSH in the absence of GSNO and PDI does not generate a signal; lane 7 shows that 3μM GSH is insufficient to interfere with nitrosylation, concurring with the findings of Sliskovic et al.[37]. The coloured molecular weight markers on the blot are shown on the left (BLUeye prestained protein ladder, 2.5 μL, Geneflow).

j, Identification of LC1 in somite extract (25µg protein); the blot was cut in half above the 41K marker and the top half of the membrane was probed with rabbit anti-tubulin followed by goat anti-rabbit IgG; the bottom half was probed with mouse monoclonal antibody against amino acids 2257-2357 of mouse MAP-1B (LC1) followed by goat anti-mouse IgG. The molecular weight markers on the blot are shown to the right (BLUeye prestained protein ladder, 3µl).
k, Identification of LC1 as a substrate for S-nitrosylation; cell-free somite extract (200µg) was treated with D-NAME or L-NAME, followed by further incubation in GSNO (200µM), as described in the Methods. Samples were then processed for the presence of S-nitrosylated proteins using iodo-TMT as described in the Methods. Protein samples (15µg) were then fractionated and blotted, after which the blot was cut as described for Fig. 3j. The top half was treated with anti-tubulin and the bottom half with anti-iodoTMT. L-NAME treatment blocked S-nitrosylation, as shown by the lack of iodoTMT labelling. The control D-NAME was without effect.

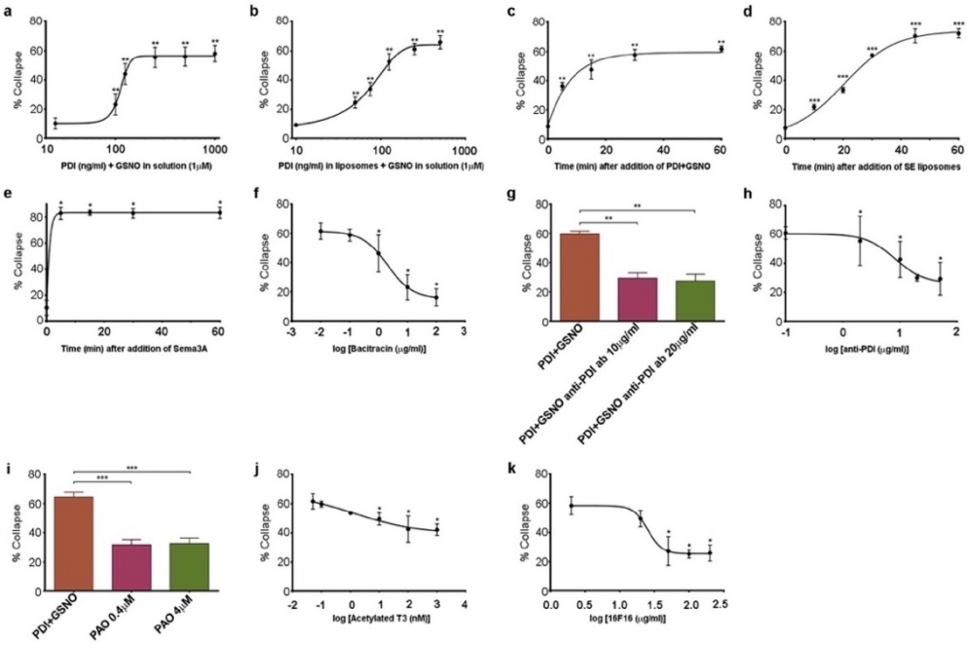

Figure 3-figure supplement 3

a,b, Comparison of collapse induced by PDI+GSNO either in solution (a) or in liposomes (b) when PDI is applied at a range of concentrations together with GSNO (1μM).

c-e, Comparison of collapse time course after applying PDI (125ng/ml) and GSNO (1μM) in solution (c), after SE in liposomes (d), and after Sema3A (e).

f-k, Assays testing purified bacitracin (f), anti-PDI neutralizing antibody (g,h), PAO (i), T3 (j) and 16F16 (k) on PDI+GSNO-induced collapse.

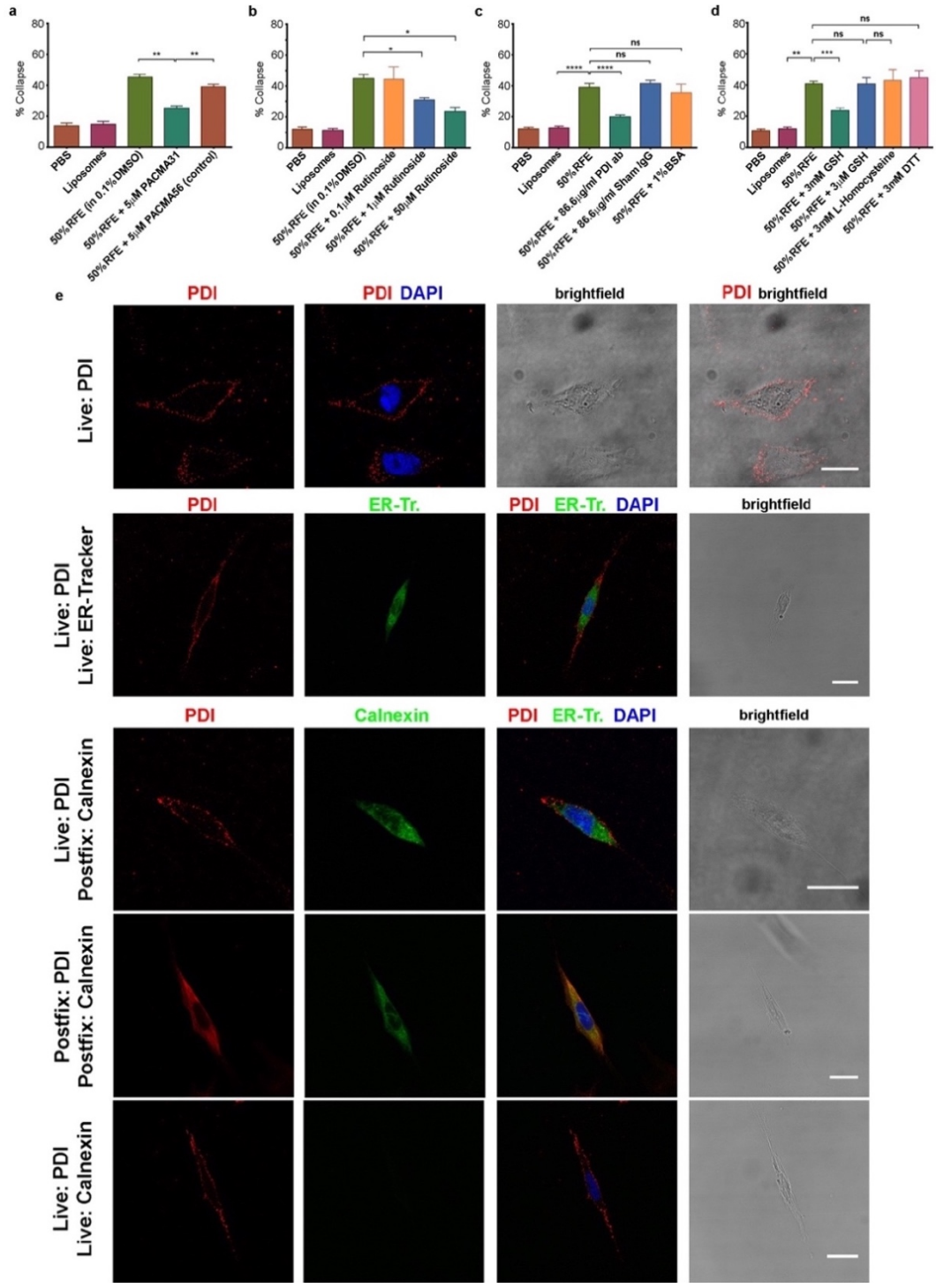

Figure 4

csPDI activity in mammalian forebrain

a-d, Collapse assays using PACMA 31 and PACMA 56 (a), quercetin-3-O-rutinoside (b), immunodepletion (c), and reducing agents (d).

e, Immunocytochemistry on live human astrocytic (1718) cells. Scale bars 20μM. Row 1, anti-PDI (red) shows PDI expression at the cell surface, DAPI-staining (blue) shows position of nucleus. Row 2, anti-PDI live staining at the cell surface (red) contrasts with selective staining of ER with ER-Tracker (green). Rows 3,4, fixation permits visualisation of ER-PDI using anti-calnexin (green), which is absent under live staining conditions (Row 5).

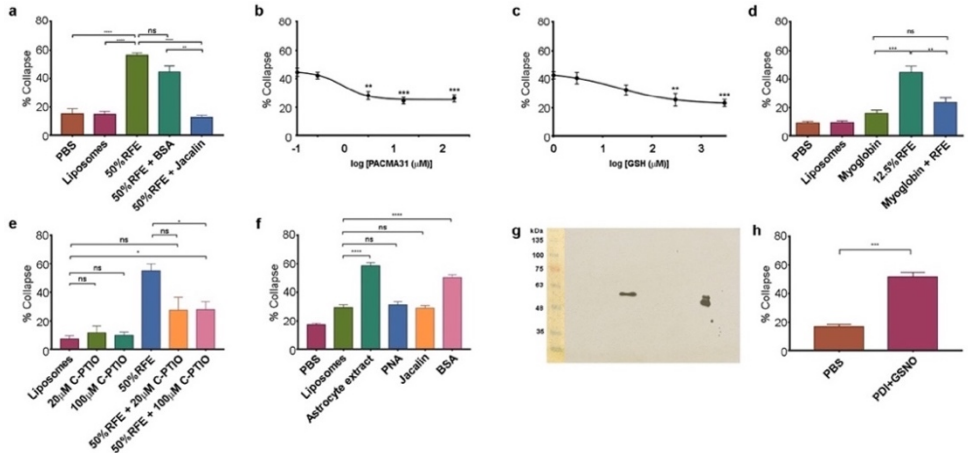

Figure 4-figure supplement 4

a, Collapse assays showing depletion of collapse activity in rat forebrain extract (RFE) by use of immobilized jacalin; immobilized BSA was used as an additional control.

b, Collapse assays showing quantification of PACMA31 dose/response relationship.

c, Collapse assay and GSH titration.

d, Collapse assays testing the NO scavenger myoglobin (20μM).

e, Collapse assays testing the NO scavenger C-PTIO.

f, Collapse assays using dialysed extracts from human 1718 astrocytic cells, testing activity before and after depletion by immobilized PNA and jacalin; immobilized BSA was used as an additional control.

g, Western blot of rat cortical astrocyte cell surface preparation using anti-PDI antibody, showing one band at 57KDa in the centre of the blot. The doublet (right) is control purified bovine PDI (500ng), and the lower band indicates that this control sample was partially oxidised. Molecular weight markers (10μl; BLUeye Prestained Wide Range Protein ladder, Geneflow) are shown (left), transferred from the gel to the blot.

h, Collapse assays testing reactivity of chick retinal axon growth cones to PDI+GSNO.

SUPPLEMENTARY TABLE 1

Figure	Treatment	# replicates (n)	Test	Value	Test	Value
1b-f	Representative images of 15 replicates	15				
ED 1b	128nM PDI: 7 determinations, 3 enzyme batches; 64nM PDI: 7 determinations, 5 enzyme batches; 32nM PDI: 5 determinations, 3 enzyme batches; 12nM PDI + PNA agarose: 4 determinations, 2 enzyme batches, 2 PNA-agarose batches		Two-way RM ANOVA > Bonferroni's multiple comparison test	F(10, 90) = 0.7658, p=0.661 (post-hoc, p > 0.999 all comparisons)		
2a	Representative image of siRNA-injected embryos	331				
2b	*n* = 144 embryos	144				
2c,d	*n* = 24/149 embryos showed abnormal phenotype	149				
2e,f	PACMA31: *n* = 14/29 embryos abnormal phenotype	29				
2g	PACMA56: *n* = 19/20 embryos normal phenotype	20				
ED 2a-d	Representative images of 15 replicates	15				
ED 2e-g	Representative images of 4 replicates	4				
ED 2h	Representative images of 6 replicates	6				
ED 2i	siRNA	9				
	siRNA + 1µg plasmid	10	Mann-Whitney test (vs siRNA)	p = 0.0028		
	siRNA + 2µg plasmid	9	Mann-Whitney test (vs siRNA)	p = 0.0019		
ED 2l	Ventral root, PACMA 31	8	Mann-Whitney test (vs PACMA 56)	p < 0.01		
	Ventral root, PACMA 56	10				
ED 2n	Dorsal bridges, PACMA 31	8	Mann-Whitney test (vs PACMA 56)	p < 0.001		
	Dorsal bridges, PACMA 56	10				
ED 2o	Ventral root width, PACMA 31	12	Mann-Whitney test (vs PACMA 56)	p < 0.001		
	Ventral root width, PACMA 56	9				
	Ventral root, uninjected side	10				
COLLAPSE ASSAYS						
3a	PBS	6	1-way ANOVA Kruskal-Wallis test	p = 0.482		
	Liposomes	7				
	PDI 25ng/ml	3				
	PDI 50ng/ml	3				
	PDI 100ng/ml	3				
	PDI 500ng/ml	3				
	PDI 1000ng/ml	3				
3b	PBS	10				
	PDI (125ng/ml)	8	Mann-Whitney test (vs PBS)	p < 0.0001		
	GSNO (1µM)	8	Mann-Whitney test (vs PBS)	p < 0.0001		
	PDI+GSNO	10	Mann-Whitney test (vs PBS)	p < 0.0001		
3c	PBS	8				
	Liposomes	7				
	Somite extract (SE)	12				
	SE + 5µM PACMA 31	18	Mann-Whitney test (vs SE)	p < 0.0001		
	SE + 5µM PACMA 56	11	Mann-Whitney test (vs SE)	p = 0.137	Mann-Whitney test (vs PACMA31)	p < 0.0001
3d	PBS	7	Mann-Whitney test (vs PDI+GSNO)	p = 0.003		
	DTT (3mM)	4	Mann-Whitney test (vs PDI+GSNO)	p = 0.0016		
	PDI+GSNO	8				
	L-homocysteine (3mM)	4	Mann-Whitney test (vs PDI+GSNO)	p = 0.0016		
	PDI+GSNO	8				
	PDI+GSNO + GSH (3µM)	4				
	PDI+GSNO + GSH (3mM)	5	Mann-Whitney test (vs PDI+GSNO)	p = 0.004		
	PDI+GSNO + DTT (3mM)	6				
	PDI+GSNO + L-homocysteine (3mM)	6	Mann-Whitney test (vs L-homocysteine (3mM)	p = 0.002		
3e	PBS	4				
	Dialysis supernatant	3	Mann-Whitney test (vs Dialysis supernatent)	p = 0.40		
	SE	7	Mann-Whitney test (vs PBS)	p = 0.0061	Mann-Whitney test (vs Dialysis supernatant)	p = 0.0167
	SE + GSH (3mM)	5	Mann-Whitney test (vs PBS)	p = 0.0159	Mann-Whitney test (vs SE)	p = 0.0025
	SE + L-homocysteine	5	Mann-Whitney test (vs SE)	p = 0.3434	Mann-Whitney test [vs SE + GSH (3.3mM)]	p = 0.0079
3f	PBS	9	Mann-Whitney test (vs SE)	p = 0.0142		
	Liposomes	9	Mann-Whitney test (vs PDI+GSNO)	p < 0.0001	Mann-Whitney test (vs SE)	p = 0.0012
	PDI+GSNO	8	Mann-Whitney test [vs SE + myoglobin (20µM)]	p = 0.036		
	PDI+GSNO + myoglobin	12	Mann-Whitney test (vs PDI+GSNO)	p < 0.0001	Mann-Whitney test [vs SE + myoglobin (20µM)]	p = 0.0019
	SE	9	Mann-Whitney test (vs PDI+GSNO + myoglobin)	p = 0.0009	Mann-Whitney test [vs PDI+GSNO + SE + myoglobin (20µM)]	p = 0.040
	SE + myoglobin (20µM)	9	Mann-Whitney test (vs Liposomes)	p = 0.0005		
3g	PBS	6	Mann-Whitney test (vs PDI+GSNO)	p = 0.0043		
	GSNO (1µM)	4	Mann-Whitney test (vs PBS)	p > 0.999		
	PDI (500ng/ml)	4	Mann-Whitney test (vs PBS)	p = 0.257		
	PDI+GSNO	6	Mann-Whitney test (vs PDI+GSNO + C-PTIO)	p = 0.013		
	C-PTIO (20µM)	6				
	C-PTIO + GSNO	6				
	PDI + C-PTIO	6				
	PDI+GSNO + C-PTIO	6	Mann-Whitney test (vs PBS)	p = 0.132		
3h	PBS	11				
	Liposomes	14				
	PBS + L-NAME	10	Mann-Whitney test (vs PBS)	p = 0.2437		
	PBS + D-NAME	7	Mann-Whitney test (vs PBS)	p = 0.2463	Mann-Whitney test (vs PBS + L-NAME)	p = 0.906
	SE	9				
	SE + L-NAME	15	Mann-Whitney test (vs SE)	p = 0.0009		
	SE + D-NAME	4	Mann-Whitney test (vs SE)	p = 0.3958		
	Calcimycin	5				
ED 3a	Each PDI concentration	3 or 5				
ED 3b	Each PDI concentration	4				
ED 3c	Each time point	6				
ED 3d	Each time point	3 or 4				
ED 3e	Each time point	3 or 4				
ED 3f	Each PDI concentration	3-5				
ED 3g	PDI+GSNO	4				
	PDI+GSNO + ab (10µg/ml)	8	Mann-Whitney test (vs PDI+GSNO)	p = 0.0040		
ED 3h	Each PDI concentration	3-6				
ED 3i	PDI+GSNO	9				
	PAO (0.4µM)	7	Mann-Whitney test (vs PDI+GSNO)	p = 0.0002		
	PAO (4µM)	8	Mann-Whitney test (vs PDI+GSNO)	p < 0.0001		
ED 3j	Each T3 concentration	3 or 4				
		6				
ED 3k	Each 16F16 concentration	3				
4a	PBS	7				
	Liposomes	8				
	RFE (50%)	10	Mann-Whitney test [vs RFE + PACMA31 (5µM)]	p < 0.0001		
	RFE + PACMA31 (5µM)	17				
4b	PBS	14				
	Liposomes	15				
	RFE (50%)	33				
	RFE + Rutinoside (0.1µM)	26				
	RFE + Rutinoside (1µM)	4	Mann-Whitney test [vs RFE (50%)]	p = 0.0292		
	Rutinoside (50µM)	6	Mann-Whitney test [vs RFE (50%)]	p = 0.0100		
4c	PBS	13				
	Liposomes	18				
	RFE (50%)	18	Mann-Whitney test (vs Liposomes)	p < 0.0001		
	RFE + anti-PDI	22	Mann-Whitney test [vs RFE (50%)]	p < 0.0001		
	RFE + IgG	20	Mann-Whitney test [vs RFE (50%)]	p = 0.3651		
	RFE + BSA	10	Mann-Whitney test [vs RFE (50%)]	p = 0.5478		
4d	PBS	17				
	Liposomes	18				
	RFE (50%)	18	Mann-Whitney test (vs Liposomes)	p < 0.0001		
	RFE + GSH (3mM)	20	Mann-Whitney test [vs RFE (50%)]	p < 0.0001		
	RFE + GSH (3µM)	6	Mann-Whitney test [vs RFE (50%)]	p = 0.7603		
	RFE + GSH + L-homocysteine (3mM)	7	Mann-Whitney test [vs RFE + GSH (3µM)]	p = 0.9452		
	RFE + DTT (3mM)	12	Mann-Whitney test [vs RFE (50%)]	p = 0.8595		
4e	Representative images of 3 replicates					
ED 4a	PBS	14	Mann-Whitney test (vs Liposomes)	p < 0.0001		
	Liposomes	25	Mann-Whitney test [vs RFE (50%)]	p < 0.0001		
	RFE (50%)	36				
	RFE + BSA	9				
	RFE + Jacalin	40				
ED 4b	Each PACMA31 concentration	5-20				
ED 4c	Each GSH concentration	6-19				
ED 4d	PBS	9				
	Liposomes	12				
	RFE	8	Mann-Whitney test (vs Myoglobin)	p < 0.0001		
	RFE + myoglobin	14	Mann-Whitney test (vs RFE)	p = 0.0022		
	Myoglobin	15	Mann-Whitney test (vs RFE + myoglobin)	p = 0.0714		
ED 4e	Liposomes	5	Mann-Whitney test [vs C-PTIO (20µM)]	p = 0.8329		
	C-PTIO (20mM)	8				
	C-PTIO (100mM)	6	Mann-Whitney test (vs Liposomes)	p = 0.5368		
	RFE	6	Mann-Whitney test [vs RFE + C-PTIO (20µM)]	p = 0.0519		
	RFE + C-PTIO (20µM)	5	Mann-Whitney test (vs Liposomes)	p = 0.0556		
	RFE + C-PTIO (100µM)	7	Mann-Whitney test (vs Liposomes)	p = 0.0101	Mann-Whitney test (vs RFE)	p = 0.0140
ED 4f	PBS	34				
	Liposomes	45				
	1718 cell extract	37	Mann-Whitney test (vs Liposomes)	p < 0.0001		
	1718 extract + PNA	32	Mann-Whitney test (vs Liposomes)	p = 0.3934		
	1718 extract + Jacalin	27	Mann-Whitney test (vs Liposomes)	p = 0.8714		
	1718 extract + BSA	53	Mann-Whitney test (vs Liposomes)	p < 0.0001		
ED 4h	PBS	10				
	PDI (500ng/ml)+GSNO (1µM)	11	Mann-Whitney test (vs PBS)	p < 0.0001		